

The Critical Beta-splitting Random Tree II: Overview and Open Problems

David J. Aldous* Svante Janson†

July 4, 2024

Abstract

In the critical beta-splitting model of a random n -leaf rooted tree, clades are recursively (from the root) split into sub-clades, and a clade of m leaves is split into sub-clades containing i and $m - i$ leaves with probabilities $\propto 1/(i(m - i))$. Study of structure theory and explicit quantitative aspects of the model is an active research topic, and this article provides an extensive overview what is currently known. For many results there are different proofs, probabilistic or analytic, so the model provides a testbed for a “compare and contrast” discussion of techniques. We give some proofs that are not currently available elsewhere, and also give heuristics for some proven results and for some open problems. Our discussion is centered around three “foundational” results.

(i) There is a canonical embedding into a continuous-time model, that is a random tree $\text{CTCS}(n)$ on n leaves with real-valued edge lengths, and this model turns out more convenient to study. The family $(\text{CTCS}(n), n \geq 2)$ is consistent under a “delete random leaf and prune” operation. That leads to an explicit inductive construction of $(\text{CTCS}(n), n \geq 2)$ as n increases, and then to a limit structure $\text{CTCS}(\infty)$ formalized via exchangeable partitions, in some ways analogous to the Brownian continuum random tree.

(ii) There is a CLT for leaf heights, and the analytic proof can be extended to provide surprisingly precise analysis of other height-related aspects.

(iii) There is an explicit description of the limit *fringe distribution* relative to a random leaf, whose graphical representation is essentially the format of the cladogram representation of biological phylogenies.

Many open problems remain.

*Department of Statistics, 367 Evans Hall # 3860, U.C. Berkeley CA 94720; aldousdj@berkeley.edu; www.stat.berkeley.edu/users/aldous.

†Department of Mathematics, Uppsala University, P.O.Box 480, SE-751 06 Uppsala Sweden; svante.janson@math.uu.se; www.math.uu.se/~svante.

1 Introduction

This article describes the current state of active research on a certain random tree model. The model arose as a toy model for phylogenetic trees, designed to mimic the uneven splits observed in real world examples (see section 4.3). The model turns out to have a rich mathematical structure. There are many questions one can ask (in addition to those suggested by the phylogenetic context), and many different proof techniques can be exploited. Indeed two of the foundational results (Theorems 2 and 5) each have three or four different proofs, probabilistic or analytic, so the model provides a testbed for a “compare and contrast” discussion of techniques.

Sections 2 - 5 state and discuss results, without proofs but with some heuristics. Proofs that are currently available in journal articles or other preprints will not be repeated. Section 6 contains those proofs not available elsewhere. Further scattered remarks are in section 7. Open problems are noted throughout, and enumerated separately as Open Problems 1 - 15.

2 The critical beta-splitting model of random trees

For $m \geq 2$, consider the distribution $(q(m, i), 1 \leq i \leq m - 1)$ constructed to be proportional to $\frac{1}{i(m-i)}$. Explicitly

$$q(m, i) = \frac{m}{2h_{m-1}} \cdot \frac{1}{i(m-i)}, \quad 1 \leq i \leq m - 1, \quad (1)$$

where h_{m-1} is the harmonic sum $\sum_{i=1}^{m-1} 1/i$. Now fix $n \geq 2$. Consider the process of constructing a random tree by recursively splitting the integer interval $[n] = \{1, 2, \dots, n\}$ of “leaves” as follows. First specify that there is a left edge and a right edge at the root, leading to a left subtree which will have the L_n leaves $\{1, \dots, L_n\}$ and a right subtree which will have the $R_n = n - L_n$ leaves $\{L_n + 1, \dots, n\}$, where L_n (and also R_n , by symmetry) has distribution $q(n, \cdot)$. Recursively, a subinterval with $m \geq 2$ leaves is split into two subintervals of random size from the distribution $q(m, \cdot)$. Continue until reaching intervals of size 1, which are the leaves. That is a discrete time construction, which we call¹ DTCS(n). Figure 1 (left) illustrates schematically the construction as interval-splitting, with the natural tree structure shown in Figure 1 (center and right).

This discrete time model was introduced and briefly studied many years ago in [6]. A more recent observation was that an associated continuous time model has appealing structural properties, and that was major motivation for the current project.

¹DTCS and CTCS are abbreviations for Discrete Time Critical Splitting and Continuous Time Critical Splitting, for reasons explained in section 4.3.

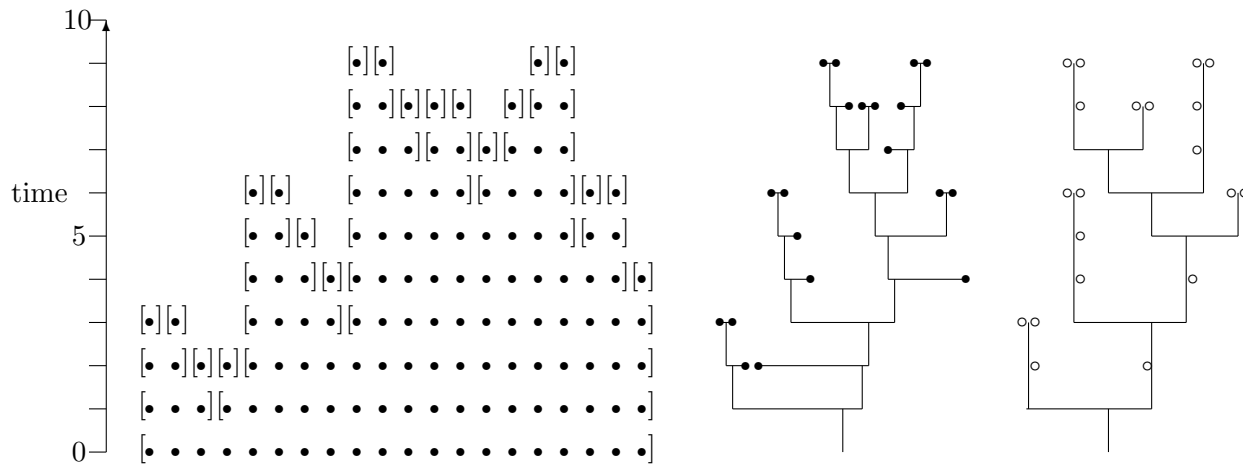


Figure 1: Equivalent representations of a realization of DTCS(20).

We define the associated continuous time model $CTCS(n)$, by declaring that an interval with $m \geq 2$ leaves is split at rate h_{m-1} , that is after an $Exponential(h_{m-1})$ random time. Figure 2 shows a schematic realization of $CTCS(20)$ as a “continuization” of the realization of $DTCS(20)$ in Figure 1. Figure 3 shows an actual realization of $CTCS(400)$.

Observe that there is no direct connection between the model (discrete or continuous) for n and the model for $n + 1$. Because a binary tree on n leaves has $n - 1$ splits, one imagines that as n increases the trees will tend to get taller. However in the continuous model there is an offsetting feature, that the initial splitting rate h_{n-1} is increasing with n . This turns out to have the following remarkable effect.

Proposition 1 *Let B_n denote the height of the branchpoint between the paths to two uniform random distinct leaves of $CTCS(n)$. Then, for each $n \geq 2$, B_n has exactly $Exponential(1)$ distribution.*

The short stochastic calculus proof will be given in section 6.1. This result hints at the “consistency” result (Theorem 7) and suggests that h_{n-1} is the canonical choice of splitting rates for the continuization.

We do find it convenient to adopt the biological term *clade* for the set of leaves in a subtree, that is the elements in a subinterval somewhere in the interval-splitting process. So the path from the root to the distinguished leaf 11 in Figure 2 passes through successive clades

$[[1, 20]]$, $[[4, 20]]$, $[[5, 20]]$, $[[9, 20]]$, $[[9, 19]]$, $[[9, 17]]$, $[[9, 13]]$, $[[9, 11]]$, $[[11]]$

which have successive sizes (number of leaves) 20, 17, 16, 12, 11, 9, 5, 3, 1.

Regarding terminology, remember that “time” and “height” are the same, within

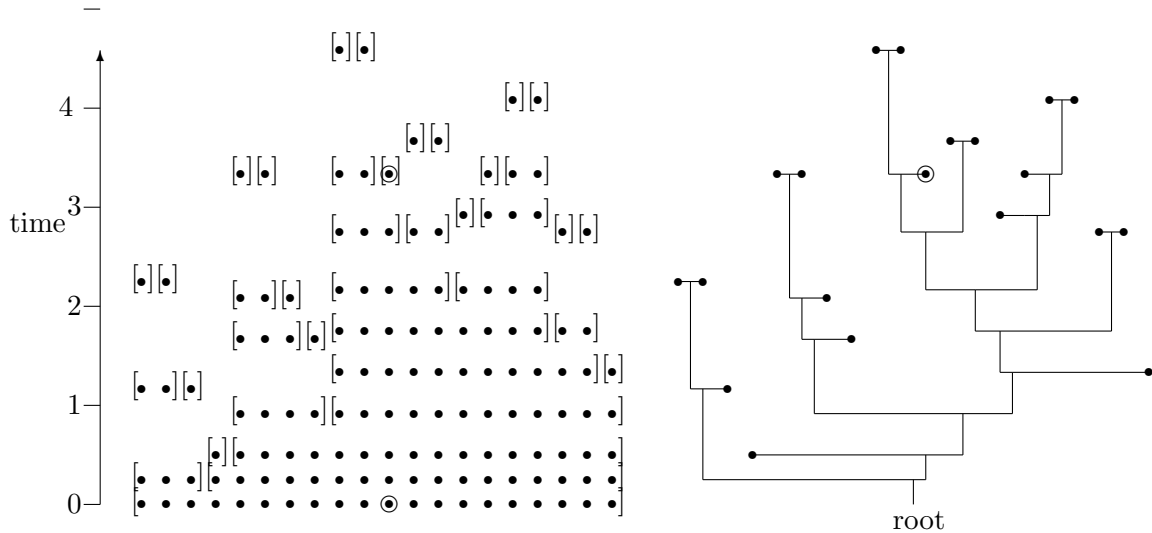


Figure 2: Equivalent representations of a realization of $\text{CTCS}(20)$. One distinguished leaf is marked.

the construction of $\text{CTCS}(n)$ for fixed n . The height² of a leaf is the time at which its clade becomes a singleton, and the height of a split between clades is the time at which the split occurs. Within the mathematical analysis of random processes we generally follow the usual “time” convention, while in stating results we generally use the tree-related terminology of “height”.

2.1 The three foundational results

We regard the following three results as “foundational”, in that they open the way to further developments.

- In section 3 we describe the CLT for leaf heights, Theorem 2, leading to results and conjectures for other height-related statistics.
- In section 4 we describe the “occupation measure” Theorem 5, leading to an explicit description of the asymptotic *fringe process*, many of whose properties have yet to be investigated. The fringe process is essentially the way that real-world phylogenies are drawn as *cladograms*, and we illustrate a real example alongside a realization of our model.
- In section 5 we describe the consistency property (Theorem 7) and the resulting representation of a limit tree $\text{CTCS}(\infty)$ via an exchangeable random partition

²Or depth, if one draws trees upside-down.

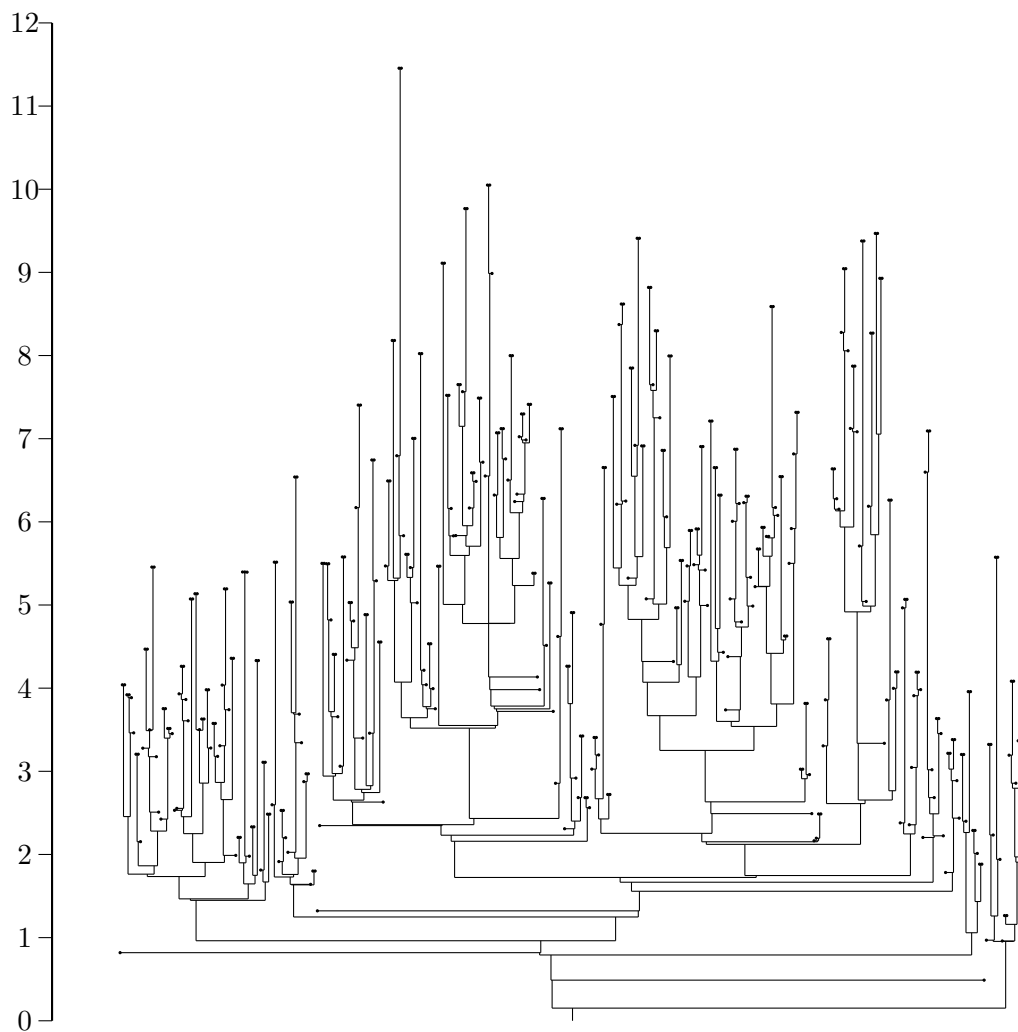


Figure 3: A realization of the tree-representation of the CTCS(n) model with $n = 400$. Drawn as in the previous Figure, so the width of subtrees above a given time level are the sizes of clades at that time.

of \mathbb{N} . This leads to a description of the “number of subclades along a path to a uniform random leaf on the infinite boundary” process within $\text{CTCS}(\infty)$ in terms of a certain subordinator (Theorem 12), and the possibility for further analysis of $\text{CTCS}(\infty)$ itself.

We should emphasize that, since the first arXiv version of this article, Alexander Iksanov has found more concise proofs [37, 36] of the first two results, briefly mentioned later. In section 7.3 we discuss analogies with the Brownian continuum random tree.

3 Heights and related statistics

To start our study of quantitative aspects of $\text{CTCS}(n)$, let us consider heights of leaves. What can we say about the height D_n of a uniform random leaf ℓ ? Figure 3 suggests that D_n increases slowly with n .

3.1 The harmonic descent chain

We can characterize D_n in an alternate way, as follows. In the discrete construction, the sequence of clade sizes along the path from the root to ℓ is the discrete-time Markov chain, starting in state n , whose transition ($m \rightarrow i$) probabilities $q^*(m, i)$ are obtained by size-biasing the $q(m, \cdot)$ distribution; so

$$q^*(m, i) := \frac{2i}{m}q(m, i) = \frac{1}{h_{m-1}} \frac{1}{m-i}, \quad 1 \leq i \leq m-1, \quad m \geq 2 \quad (2)$$

from (1). Because the continuous-time CTCS process exits m at rate h_{m-1} , the continuous-time process of clade sizes as one moves at speed 1 along the path is the continuous-time Markov process on states $\{1, 2, 3, \dots\}$ with transition rates

$$\lambda_{m,i} = \frac{1}{m-i}, \quad 1 \leq i \leq m-1, \quad m \geq 2 \quad (3)$$

with state 1 absorbing. So D_n is the absorption time for this chain, started at state n . Let us call this the (continuous-time) *harmonic descent* (HD) chain.³

There is a simple probabilistic heuristic for the behavior of the harmonic descent chain, leading to the approximation (4) below. Write $\mathbf{X} = (X_t, t \geq 0)$ for the HD chain with rates (3), or $\mathbf{X}^{(n)} = (X_t^{(n)}, t \geq 0)$ for this chain starting with $X_0^{(n)} = n$. The key idea is to study the process $\log \mathbf{X} = (\log X_t, t \geq 0)$. By considering its transitions (see section 6.2.1) one quickly sees that, for large n , there should be a good approximation

$$\log X_t^{(n)} \approx \log n - Y_t \text{ while } Y_t < \log n \quad (4)$$

³*Descent* is a reminder that the chain is decreasing. Despite its simple form, the HD chain has apparently never been studied before.

where $(Y_t, 0 \leq t < \infty)$ is the subordinator with *Lévy measure* ψ_∞ and corresponding σ -finite density f_∞ on $(0, \infty)$ defined as

$$\psi_\infty[a, \infty) := -\log(1 - e^{-a}); \quad f_\infty(a) := \frac{e^{-a}}{1 - e^{-a}}, \quad 0 < a < \infty. \quad (5)$$

Recall that a *subordinator* [11] is the continuous-time analog of the discrete-time process of partial sums of i.i.d. positive summands: informally

$$\mathbb{P}(Y_{t+dt} - Y_t \in da) = f_\infty(a) da dt.$$

Such a subordinator satisfies the law of large numbers

$$t^{-1}Y_t \rightarrow \rho \text{ a.s. as } t \rightarrow \infty \quad (6)$$

where the limit is the mean

$$\rho = \int_0^\infty \psi_\infty[a, \infty) da = \int_0^\infty -\log(1 - e^{-a}) da = \pi^2/6. \quad (7)$$

Moreover the subordinator satisfies a central limit theorem, because the central limit theorems for sums of i.i.d. variables and for renewal processes⁴ extend immediately to subordinators by considering integer times. By calculating the variance of the subordinator, see (41) in section 6.2.1, one anticipates (assuming the approximation (4) is sufficiently accurate) the following CLT.⁵

Theorem 2

$$\frac{D_n - \mu \log n}{\sqrt{\log n}} \rightarrow_d \text{Normal}(0, \mu^3 \sigma^2) \text{ as } n \rightarrow \infty$$

where

$$\mu := 1/\zeta(2) = 6/\pi^2 = 0.6079\dots; \quad \sigma^2 := 2\zeta(3) = 2.4041\dots$$

Figure 4 shows the Normal distribution emerging.

3.2 Proofs of the CLT for leaf height

We currently know 4 proofs of Theorem 2, described below in chronological order of discovery.

Proof 1. The first proof we found, given for the record in section 6.2, is a direct attempt to justify the approximation (4) so that one can apply a martingale CLT. This is in principle straightforward but seems quite tedious and lengthy in detail.

⁴Commonly seen as a textbook exercise, e.g. [29] 10.6.3 or [17] 3.4.7.

⁵Euler's formula $\zeta(2) := \sum_{i \geq 1} i^{-2} = \pi^2/6$ is used frequently in proofs.

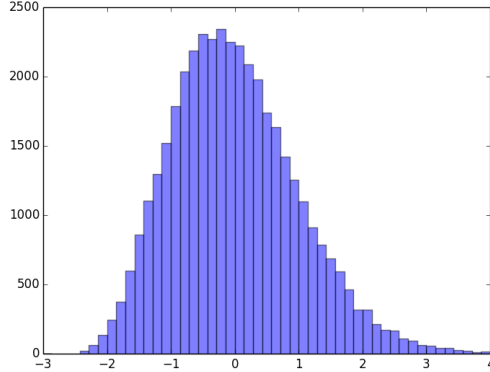


Figure 4: Histogram of leaf heights, relative to mean and s.d.; multiple simulations with $n = 3,200$.

Proof 2. The second proof we found is via an analysis of recursions for the Laplace transforms of D_n . The full proof (and many other results indicated later) by this methodology appears in the article [8]. To illustrate that methodology, in section 6.3 we show (following the first steps of a proof in [8]) how to prove

$$\mathbb{E}[D_n] = \frac{6}{\pi^2} \log n + O(\log \log n) \text{ as } n \rightarrow \infty. \quad (8)$$

Proof 3. The simple form (3) of the transitions suggests that the HD chain might have arisen previously in some different context, but we have not found any reference. However there is a general *contraction method* [49] which has been used to prove convergence in distribution for other recursively-defined structures. Kolesnik [41] uses that method to prove Theorem 2.

Proof 4. Iksanov [37] shows that Theorem 2 can be derived from known results [24] in the theory of *regenerative composition structures*. To quote [37], they “exploit a connection with an infinite “balls-in-boxes” scheme, a.k.a. Karlin’s occupancy scheme in random environment”. This is an exact relationship for finite n , unlike in previous proofs, thus allowing a shorter derivation of Theorem 2 from known results. See Section 5.5 for a brief discussion.

Why are we mentioning 4 proofs? As discussed in section 6.5, a more refined analysis of correlations between leaf-heights is needed for analysis of the tree height. It is not clear which of these techniques might be most applicable for tackling such possible extensions.

3.3 Sharper results

The analysis of recursions method, illustrated here in section 6.3 to prove (8), can be pushed much further, at the cost of substantial technical intricacy.

Theorem 3 ([8])

$$\mathbb{E}[D_n] = \frac{1}{\zeta(2)} \log n + O(1) \quad (9)$$

$$\text{var}(D_n) = (1 + o(1)) \frac{2\zeta(3)}{\zeta^3(2)} \log n. \quad (10)$$

And even sharper results hold under a certain *h-ansatz* described in [8].

Recall that our D_n refers to the height of a leaf in CTCS(n), that is the sum of edge-lengths on the path leading to the leaf. One can instead consider the number of edges, that is the *hop-length* L_n or equivalently the height in the discrete-time model DTCS(n). Results parallel to Theorem 3 for L_n are given in [8]. In particular

$$\mathbb{E}[L_n] \sim \frac{1}{2\zeta(2)} \log^2 n. \quad (11)$$

Informally, this is consistent with the result $\mathbb{E}[D_n] \sim \frac{1}{\zeta(2)} \log n$ for CTCS(n), as follows. One $\log n$ factor is the initial speed-up. The factor of 2 arises because, on the scale of time ($= \log(\text{clade size})$) the relative speed in continuous time decreases linearly from 1 to 0. See also section 4.1.

3.4 What is the tree height?

Write D_n^* for the height of the random tree CTCS(n) itself, that is the maximum leaf height. It is easy to prove (section 6.4)

Proposition 4

$$\mathbb{P}(D_n^* > (2 + \varepsilon) \log n) \rightarrow 0 \text{ for all } \varepsilon > 0$$

$$\mathbb{E}[D_n^*] \leq 1 + 2 \log n.$$

It is shown in [8] that one can extend the first bound to show that there exists $\alpha > 0$ such that for all $0 < \varepsilon < 1$ we have

$$\mathbb{P}(D_n^* \geq 2(1 + \varepsilon) \log n) = O(n^{-\alpha\varepsilon}). \quad (12)$$

However, this “2” is undoubtedly not the correct constant.

Open Problem 1 *Show that $D_n^* \sim c \log n$ in probability, and identify the constant c .*

We conjecture that in fact this holds for

$$c := 1 + \mu + \mu^3 \sigma^2 / 2 = 1.878\dots \quad (13)$$

Here $\mu := 1/\zeta(2) = 6/\pi^2 = 0.6079\dots$; $\sigma^2 := 2\zeta(3) = 2.4041\dots$ as in the CLT (Theorem 2). Heuristics leading to the conjectured c are given in section 6.5.

The discrete case, that is the height of DTCS(n), is somewhat similar – see section 6.6.

4 The occupation probability and the fringe process

4.1 The occupation probability

Our second foundational result about the random tree model also involves the HD chain. Recall that this is the continuous time Markov chain with rates (3), started at state n and absorbed at state 1. The chain describes the number of descendant leaves of a vertex, as one moves at speed 1 along the path from the root to a uniform random leaf. We study the “occupation probability”, that is

$$a(n, i) := \text{probability that the chain started at state } n \text{ is ever in state } i. \quad (14)$$

So $a(n, n) = a(n, 1) = 1$. The relevance of $a(n, i)$ to the tree model is that

$$\mathbb{E}[\text{number of } i\text{-leaf subtrees of CTCS}(n)] = na(n, i)/i. \quad (15)$$

It seems very intuitive (but not obvious at a rigorous level) that the limits $a(i) = \lim_{n \rightarrow \infty} a(n, i)$ exist. Note that $\sum_{i=2}^n a(n, i)/h_{i-1}$ is just the mean absorption time $\mathbb{E}[D_n]$, so (from Theorem 3) we anticipate that, assuming the limits exist,

$$\sum_{i=2}^n \frac{a(i)}{\log i} \sim \mathbb{E}[D_n] \sim (6/\pi^2) \log n.$$

This in turn suggests⁶

$$a(i) \sim \frac{6}{\pi^2} \frac{\log i}{i}.$$

However, there seems no intuitive reason to think there should be some simple formula for the limits $a(i)$. So our second foundational result was surprising to us.

⁶And this argument explains why the constant $6/\pi^2$ must be the same in Theorems 2 and 5. Similarly one sees heuristically that $\mathbb{E}[L_n] = \sum_{i=2}^n a(n, i) \sim \sum_{i=2}^n a(i) \sim 3\pi^{-2} \log^2 n$, as stated at (11).

Theorem 5 For each $i = 2, 3, \dots$,

$$a(i) := \lim_{n \rightarrow \infty} a(n, i) = \frac{6h_{i-1}}{\pi^2(i-1)}. \quad (16)$$

And $a(1) = 1$.

We currently know 3 proofs of Theorem 5, described below in chronological order of discovery.

Proof 1. First prove by coupling that the limits $a(i)$ exist. The limits must satisfy a certain infinite set of equations; the one solution $\frac{6h_{i-1}}{\pi^2(i-1)}$ was found by inspired guesswork. Then we need only to check that the solution is unique. This is straightforward in outline, though somewhat tedious in detail. A full proof is in the current version of [7], and a simplification of that proof has been found by Luca Pratelli and Pietro Rigo (personal communication).

Proof 2. This depends on the exchangeable representation of $\text{CTCS}(\infty)$ and is given in sections 6.14 - 6.15.

Proof 3. Iksanov [36] repeats his method for proving the CLT by exploiting the exact relationship with regenerative composition structures, enabling a shorter derivation of Theorem 5 from known results in that theory.

4.2 The (limit) fringe process

To be consistent with the *cladogram* representation described below, we work here in the discrete time $\text{DTCS}(n)$ setting: the definition (14) of $a(n, i)$ is of course unchanged in discrete time.

The motivation for Theorem 5 involves the (asymptotic) *fringe tree* for the random tree model $\text{DTCS}(n)$, that is the $n \rightarrow \infty$ local weak limit of the tree relative to a typical leaf. See [3, 35] for general accounts⁷ of fringe trees, which are random locally finite trees with a distinguished leaf. It is straightforward to see that the fringe tree can be described in terms of the limits $(a(i), i \geq 1)$ as follows.

(a) The sequence of clade sizes as one moves away from the distinguished leaf is the discrete time “reverse HD” Markov chain started at state 1, whose “upward” transition probabilities $q^\uparrow(i, j)$ are derived by considering for $j > i$

$$\lim_n n^{-1} \mathbb{E}[\text{number of splits } j \rightarrow (i, j-i) \text{ or } (j-i, i) \text{ in } \text{DTCS}(n)].$$

Calculating this in both directions leads to the identity

$$i^{-1} a(i) q^\uparrow(i, j) = j^{-1} a(j) (q(j, i) + q(j, j-i))$$

⁷The general accounts take limits relative to a random *vertex*, but for our leaf-labelled trees it is more natural to use leaves. In the terminology of [3, 35] these are *extended* fringe trees.

which, from the explicit formula (16) for $a(i)$, becomes

$$\begin{aligned} q^\uparrow(1, j) &= 6\pi^{-2} \frac{1}{(j-1)(j-1)}, \quad j \geq 2 \\ q^\uparrow(i, j) &= \frac{i-1}{(j-1)(j-i)h_{i-1}}, \quad 2 \leq i < j. \end{aligned} \tag{17}$$

(b) At each such step $i \rightarrow j$, there is the sibling clade of size $j - i$, and this clade is distributed as DTCS($j - i$), independently for each step.

One can check that (17) is a probability distribution by observing

$$\sum_{j>i} \frac{1}{(j-1)(j-i)} = \sum_{j>i} \frac{1}{i-1} \left(\frac{1}{j-i} - \frac{1}{j-1} \right) = \frac{h_{i-1}}{i-1}.$$

4.3 Motivation as a phylogenetic tree model

Some motivation for the random tree model came from noticing the shape of phylogenetic trees in evolutionary biology. *Phylogenetic tree* is the general phrase for any tree-like graphical representation; *cladogram* is more specifically a leaf-labeled binary tree, illustrated⁸ by a real example in Figure 6 (bottom). Nowadays such trees are typically derived from DNA analysis of extant species⁹. There is no biological significance to the positioning of left/right branches, though in our models it is convenient to make the distinction. Our random tree model DTCS(n) is one of many probability models that have been considered for cladograms. The model was proposed in [6] in 1996 with some brief informal study then, and with little further study until the current project. The motivation for this particular model came from an observation, in the small-scale study [9], that in splits $m \rightarrow (i, m - i)$ in real-world phylogenetic trees, the median size of the smaller subtree scaled roughly as $m^{1/2}$. That data is not consistent with more classical random tree models, where the median size would be $O(\log m)$ or $\Theta(m)$, but this $m^{1/2}$ median property does hold for our particular model. Figure 6 compares a simulation of DTCS(77) with a real cladogram on 77 species; these appear visually quite similar.

Cladograms are drawn in a particular way, with the species labels on leaves in a (usually horizontal) line. This differs from the typical visualization of (mathematical) random trees, such as Galton-Watson trees, where one starts from a root and then draws successive generations. Figure 5 illustrates how to re-draw such a tree as a cladogram, in a representation where the heights of branchpoints are positioned at integer heights $1, 2, 3, \dots$. Doing this in a natural way (as in Figures 5 and 6), the height of the cladogram is equal to the height (maximum leaf height) of the

⁸In particular, a cladogram has no quantitative time-scale on the vertical axis.

⁹Published trees are essentially “best fit” to noisy data, with occasional more-than-binary splits which cannot be resolved to successive binaries.

tree in the usual successive-generations picture. So in particular, the height of the cladogram representation of $\text{DTCS}(n)$ is the tree-height studied in [8], known to be of order $\log^2 n$: this is our L_n^* in section 6.6.

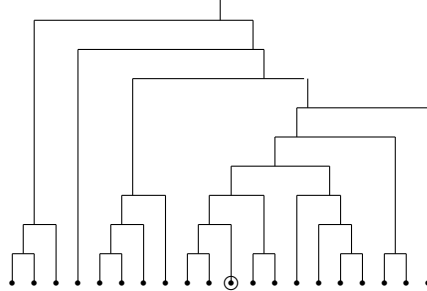


Figure 5: Cladogram representation of the Figure 1 realization of $\text{DTCS}(20)$.

The mathematical theme of [6] was to introduce the *beta-splitting model* with split probabilities

$$q(n, i) = \frac{1}{a_n(\beta)} \frac{\Gamma(\beta + i + 1)\Gamma(\beta + n - i + 1)}{\Gamma(i + 1)\Gamma(n - i + 1)}, \quad 1 \leq i \leq n - 1 \quad (18)$$

with a parameter $-2 \leq \beta \leq \infty$ and normalizing constant $a_n(\beta)$. The qualitative behavior of the model is different for $\beta > -1$ than for $\beta < -1$; in the former case the height (number of edges to the root) of a typical leaf grows as order $\log n$, and in the latter case as order $n^{-\beta-1}$. In this article we are studying the *critical case* $\beta = -1$, with two motivations.¹⁰

(a) A stochastic model, at a critical parameter value separating qualitatively different behaviors (loosely called a “phase transition” by analogy with statistical physics), often has mathematically interesting special properties: we are seeing this in the current project.

(b) Second, as mentioned above our small-scale study of real phylogenetic trees in [9] suggested that, amongst all splits of clades of size m , the median size of the smaller subclade scales roughly as $m^{1/2}$. The $\beta = -1$ case of our model has this property, immediately from the definition. More broadly, the model does seem to match qualitative features of real large phylogenetic trees. As mentioned before, Figure 6 compares a simulation of our $\beta = -1$ model with a real cladogram on 77 species; these appear visually similar. In contrast, simulations of the familiar alternative models look substantially different – see Figure 7 for the Markov model ($\beta = 0$) and the PDA model ($\beta = -1.5$).

¹⁰Hence our terminology CS for *critical splitting*. But note that *critical* in our context is quite different from the usual *critical* in the context of branching processes or percolation.

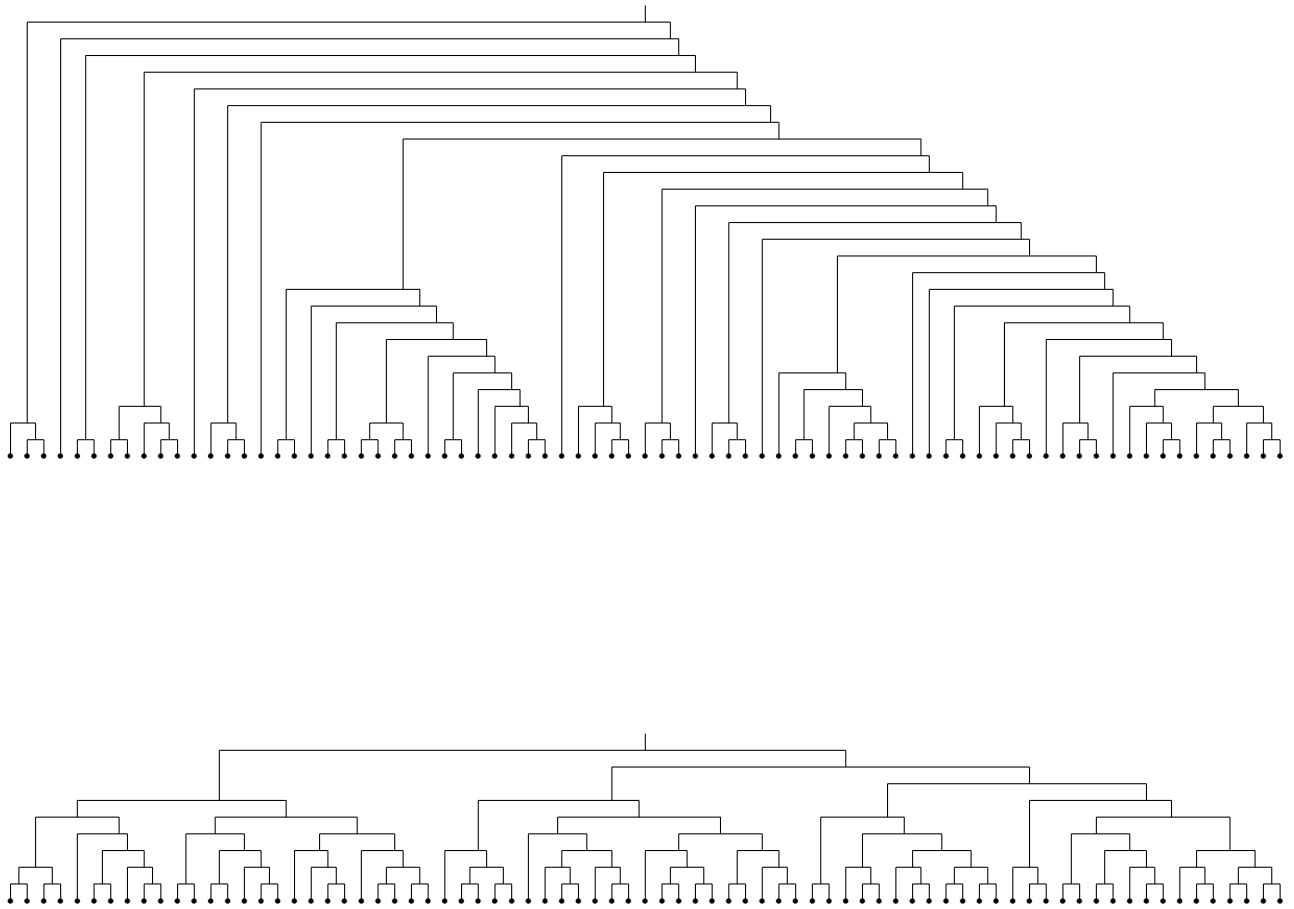


Figure 7: Simulations of the beta-splitting model on 77 species for other parameters: (top) $\beta = -1.5$; (bottom) $\beta = 0$.

As noted earlier, the general beta-splitting model is often¹¹ mentioned in the mathematical biology literature on phylogenetics as one of several simple stochastic models. See [42, 55] for recent overviews of that literature. Obviously it is biologically unsatisfactory by not being a forward-in-time model of extinctions and speciations, and indeed the latter type of model with age-dependent speciation rates is more plausible and can match the shapes of real trees quite well [32], though whether one can identify rates uniquely remains a contentious issue [51]. Is the qualitative similarity of these different models just a coincidence, or is there some mathematical connection between the models?

The recent paper [59] studies the “balance” of a leaf-labelled binary tree using a statistic which is equivalent to

$C(\text{tree}) =$ average over leaves, of number of edges from the root to the leaf.

In our model this is L_n . Consider $C(n)$, the empirical fit to $C(\text{tree})$ for n -leaf trees. The paper [59] says, based on existing data

How do real data scale? Remarkably, it is found that, over three orders of magnitude of n , there is a power-law scaling $C(n) \sim n^\eta$, with the exponent $\eta = 0.44 \pm 0.01$.

For a model that reproduces this power law, [59] suggests a model based on “niche construction”. They also have extensive references to previous work. This power law of course seems quite different from our model prediction (11) that

$$C(n) \sim \frac{1}{2\zeta(2)} \log^2 n.$$

This is perhaps an illustration of the dangers of relating asymptotics to pre-asymptotics. Figure 8 plots, over a range of n from approximately 20 to 1,000, the exact value of $\mathbb{E}[L_n]$ in our model. We see that on the log-log plot it is almost linear in n over this range: our model predicts $C(n) \approx n^{0.34}$ on this range. This indicates the difficulty in interpreting power-law relationships as justifying any particular model.

Note that our model, although designed to fit the observed balance of large clades, also gives explicit predictions for small fringe trees, as discussed below.

¹¹[6] has 317 citations on Google Scholar.

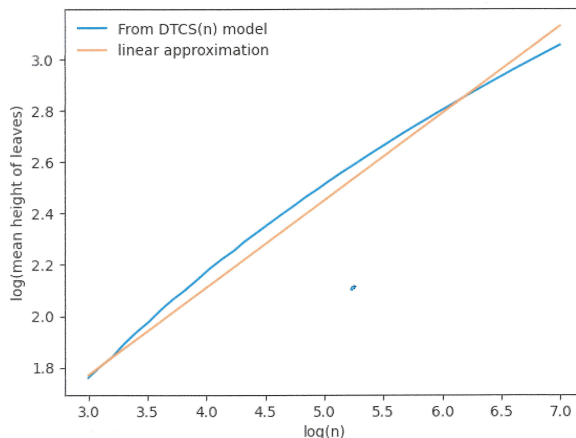


Figure 8: A log-log plot of $\mathbb{E}[L_n]$ over $20 \leq n \leq 1000$ is almost a straight line.

4.4 Properties of the fringe tree

One should visualize the fringe tree as in Figure 6, but with leaves labelled as $\dots, -2, -1, -0, 1, 2, \dots$, and with branches randomly positioned left/right instead of the biology convention of usually positioning the larger clade to the right.

There are many aspects of the fringe tree that one could study. One can study it as an interesting process in its own right – loosely analogous to a stationary process indexed by \mathbb{Z} . Recall that, in the fringe tree, the probability that a leaf is in some clade of size i equals $a(i)$. Because a clade of size i has the DTCS(i) distribution, we can then calculate the probability $p(\chi)$ that a leaf is in a specific clade χ . Some results are shown in Figure 9. In that figure we have grouped clades with the same *shape*, meaning that (as in the biology use) we do not distinguish left and right branches. Figure 9 compares these model predictions with the data from a small set of real cladograms¹² – 10 cladograms with a total of 995 species.

These results can be compared with the corresponding results for some other models of random cladograms in [40, Appendix A], see also [38]. Note that the models treated in [40] are precisely the cases $\beta = \infty, 0, -3/2$ of the beta-splitting tree [6].

But also one can use the fringe process to study asymptotics of statistics of

¹²Dragonflies [45], eagles [44], elms [57], gamebirds [13], ladybirds [47], parrots[58], primates [27], sharks [56], snakes [19], swallows [53]

DTCS(n) or CTCS(n), for statistics which depend only on the structure of the tree near the leaves. In particular, the number $N_n(\chi)$ of copies of a size- i clade χ in DTCS(n) will satisfy $n^{-1}\mathbb{E}[N_n(\chi)] \rightarrow p(\chi)/i$. By analogy with results for other random tree models – see [35] sec. 14 – and because occurrences of a given χ are only locally dependent, it should not be difficult to resolve

Open Problem 2 *Prove that $n^{-1}\text{var}(N_n(\chi))$ converges to some limit $\sigma^2(\chi)$ and that the corresponding CLT holds.*

Another example is illustrated in the next section.

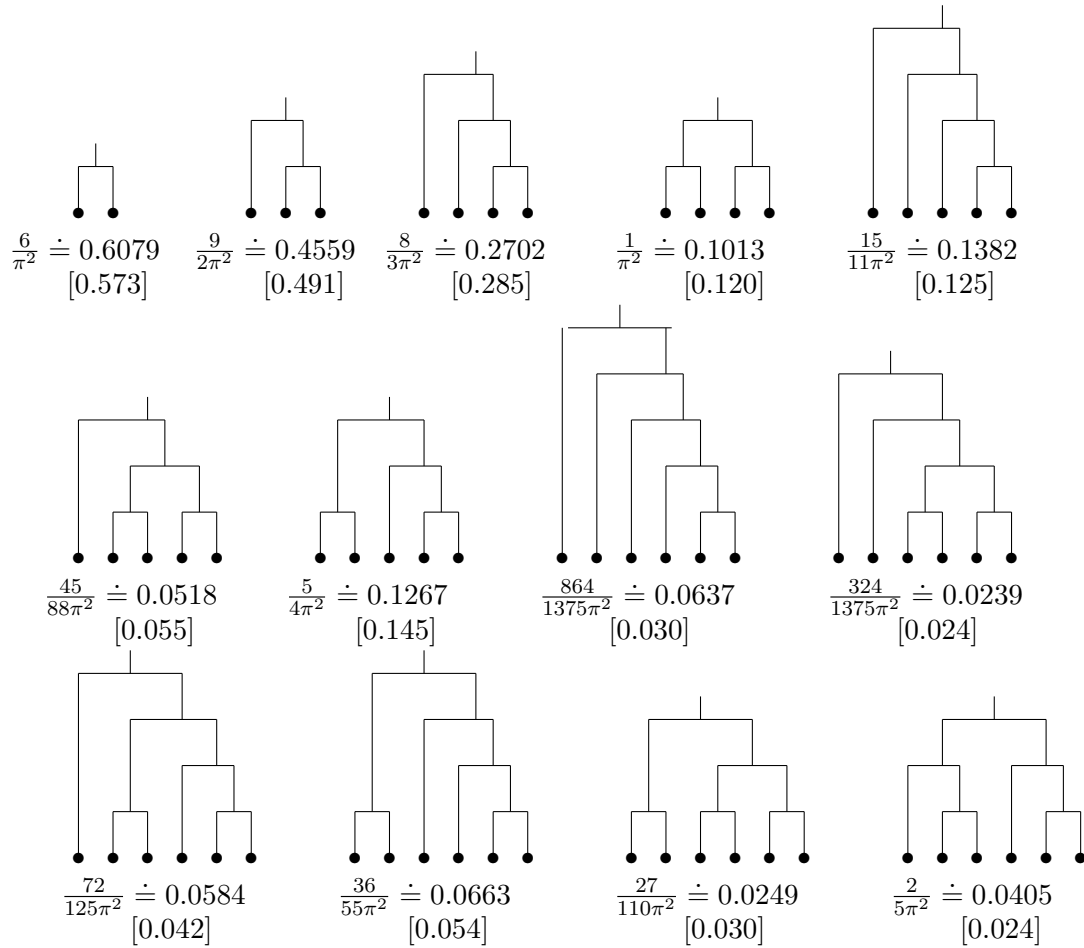


Figure 9: Proportions of leaves in clades of a given shape, for each shape with 2 – 6 leaves in the fringe process. The top number is from our model, the bottom number $[\dots]$ from our small data set.

4.5 The length of CTCS(n)

The number of edges of CTCS(n) equals $n - 1$. Identifying *length* of an edge with *duration of time*, one can consider the length Λ_n of CTCS(n), that is the sum of edge-lengths. The expectation of the number of size- i clades in CTCS(n) equals $\frac{n}{i}a(n, i)$, so we immediately have

$$\mathbb{E}[\Lambda_n] = n \sum_{i=2}^n \frac{a(n, i)}{ih_{i-1}}. \quad (19)$$

Because $\lim_n a(n, i) = a(i)$ and

$$\sum_{i=2}^{\infty} \frac{a(i)}{ih_{i-1}} = \frac{6}{\pi^2} \sum_{i=2}^{\infty} \frac{1}{i(i-1)} = \frac{6}{\pi^2} \quad (20)$$

we naturally expect

Proposition 6 $\lim_n n^{-1}\mathbb{E}[\Lambda_n] = \frac{6}{\pi^2}$.

We prove this in section 6.7. The fact that the limit equals $a(2)$ has an intriguing consequence – see section 6.10. As with the subtree counts, mentioned in section 4.4, it should not be difficult to resolve

Open Problem 3 *Prove that $n^{-1}\text{var}(\Lambda_n)$ converges to some limit σ^2 and that the corresponding CLT holds.*

4.6 Combinatorial questions

There are a range of what one might call “combinatorial” questions related to the fringe tree. What is the probability that two independent copies of DTCS(n) have the same shape? Numerics for $n \leq 200$ suggest a probability $\asymp 0.44^n$, but as in the discussion around Figure 8 we have little confidence that this is the correct asymptotics.

Regarding the number $N_n(\chi)$ of copies of a clade χ in DTCS(n), one could study distributions of the following:

Open Problem 4

- *The number $K_n := \sum_{\chi} 1_{(N_n(\chi) \geq 1)}$ of different-shape clades within (a realization of) DTCS(n).*
- *The largest clade that appears more than once within DTCS(n).*
- *The smallest clade that does not appear within DTCS(n).*

For questions like these, it would surely be helpful to have explicit bounds on how well the asymptotic fringe distribution approximates the fringe of $\text{DTCS}(n)$. This reduces to

Open Problem 5 *Find explicit bounds for $|a(n, i) - a(i)|$.*

5 The consistency property and the exchangeability representation

5.1 The consistency property

The interval-splitting construction of $\text{CTCS}(n)$ implicitly assigns leaf-labels $\{1, 2, \dots, n\}$ but conceptually we are thinking of recursively splitting a set of objects which have labels but without any prior structure on the label-set. So it is convenient to re-define $\text{CTCS}(n)$ by applying a uniform random permutation to these leaf-labels.¹³ So our “path to a uniform random leaf” is equivalent (in distribution) to “path to leaf 1”. And “delete a uniform random leaf” is equivalent to “delete leaf n ”. Now we can define a “delete a leaf, and prune” operation, illustrated in Figure 10.

Note that the length of horizontal edges in the figure has no significance; these edges serve only to indicate which are the left and right branches.

We can now state the *consistency property of CTCS*. Note that this consistency holds only for the continuous-time model, not the discrete-time model DTCS .

Theorem 7 *The operation “delete and prune leaf $n + 1$ from $\text{CTCS}(n + 1)$ ” gives a tree distributed as $\text{CTCS}(n)$.*

So we can construct an infinite *consistent growth process* ($\text{CTCS}(n), n = 1, 2, 3, \dots$) such that, for each n , “delete and prune leaf n from a realization of $\text{CTCS}(n + 1)$ ” gives exactly a realization of $\text{CTCS}(n)$. In particular, the joint distribution $(\text{CTCS}(n + 1), \text{CTCS}(n))$ will determine the associated conditional distribution of $\text{CTCS}(n + 1)$ given $\text{CTCS}(n)$, which turns out to be described by an explicit *growth algorithm*, stated below. We prove Theorem 7 in section 6.8 via explicit formulas for the distributions, which will immediately provide the required conditional distributions and growth algorithm. In section 6.9, we give an alternative, more conceptual proof with fewer calculations.

In the context of *growth* of trees, it is more evocative to use the word *buds* instead of *leaves*, which we use in the following. In Figure 10 we see *side-buds* such as a , and end *bud-pairs* such as b, c .

We start with $\text{CTCS}(1)$, which has a single bud at the root.

¹³This of course yields a certain type of (finite) exchangeability, suggesting a limit structure involving infinite exchangeability, described in section 5.3.

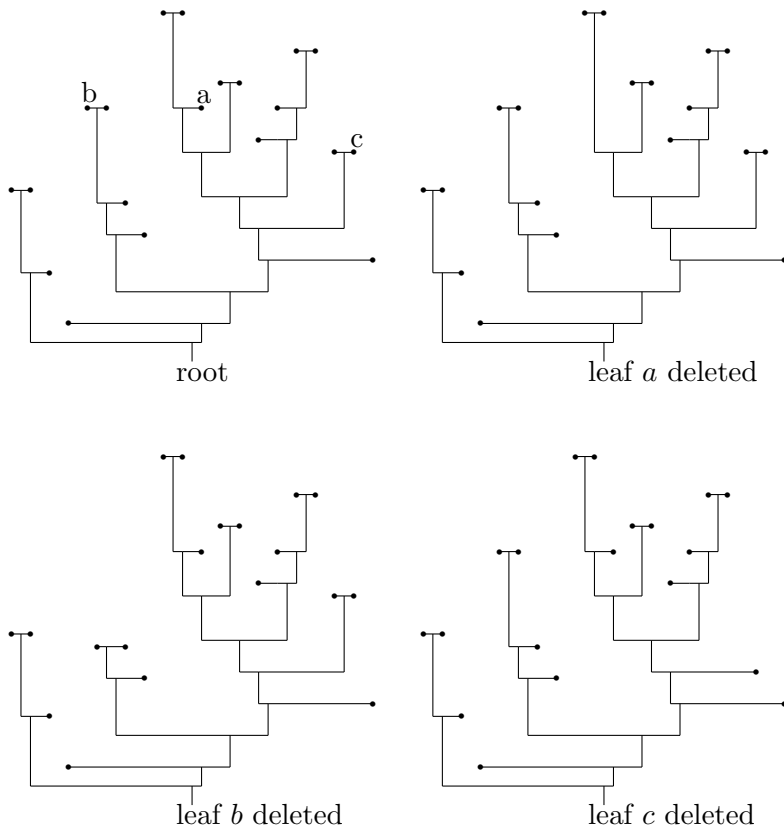


Figure 10: The delete and prune operation: effect of deleting leaf a or b or c from the top left tree.

The growth algorithm. Given a realization of $\text{CTCS}(n)$ for some $n \geq 1$:

- Pick a uniform random bud; move up the path from the root toward that bud. A “stop” event occurs at rate $= 1/(\text{size of sub-clade from current position})$.
- If “stop” before reaching the target bud, make a side-bud at that point, random on left or right.
- Otherwise, extend the target bud into a branch of $\text{Exponential}(1)$ length to make a bud-pair.

Remark 8 In our standard representations of the trees, we stop at each leaf. In what follows, it is sometimes advantageous to consider an *extended* representation where we add a vertical line to infinity from each leaf; then each leaf lies on a unique path from the root continuing up to ∞ . Using that representation, the growth algorithm has an even simpler description, where the two alternative cases above are merged into one.

We note also that the consistency property in Theorem 7 implies that the subtree spanned by two random leaves in $\text{CTCS}(n)$ (together with the root) has the same distribution as $\text{CTCS}(2)$; this gives another proof of Proposition 1.

5.2 Exploiting the growth algorithm

One might expect to be able to exploit this inductive construction to prove asymptotic results, but we have been unable to do so, yet. One possibility is outlined in section 6.10. Another possibility: the construction is reminiscent of other structures where martingales play a useful role, for instance urn models [48] and branching process and branching random walk [54], so

Open Problem 6 *Is there a useful martingale associated with the inductive construction?*

5.3 The exchangeable partitions representation

As mentioned above, a consequence of Theorem 7 is that we can construct a canonical *consistent growth process* $(\text{CTCS}(n), n = 1, 2, 3, 4, \dots)$ of random trees in which, for each n , the realization of $\text{CTCS}(n)$ is precisely the realization obtained from $\text{CTCS}(n + 1)$ via the “delete leaf $n + 1$ and prune” operation. Intuitively, there must be some kind of limit object $\text{CTCS}(\infty) := \bigcup_{n=1}^{\infty} \text{CTCS}(n)$. An insight is provided by Proposition 1 that, in $\text{CTCS}(n)$, the height of the branchpoint between two distinct random leaves has exactly Exponential(1) distribution, for each $n \geq 2$. As $n \rightarrow \infty$ these branchpoints persist, and (by the exchangeability argument for (22) below: analogous to the Pólya urn scheme) the proportion of leaves in each branch converges to a random non-zero limit. Here, as in Remark 8, we are imagining the line representing a leaf as continuing up to ∞ . So one could define the limit object $\text{CTCS}(\infty)$ as a kind of tree in which the leaves have gone off to ∞ and in which there is a unit flow from the root to infinity along the branches. However this is not the usual kind of “locally finite” infinite tree¹⁴, because a realization has a countable infinite dense set of branchpoints.

Instead of seeking to formalize $\text{CTCS}(\infty)$ as a random tree, we will use an existing formalism via Kingman’s theory of exchangeable partitions. A standard reference is [11] section 2.3 – see also [10] and [52] Chapter 2. Applications to tree models somewhat similar to ours, though emphasizing characterizations rather than our explicit calculations, have been given in [31] (see section 7.3 for further discussion). The key feature of this approach is the *paintbox theorem*, developed below.

Fix a level (time) $t \geq 0$. Cutting the tree $\text{CTCS}(n)$ at level t yields a partition $\Pi^{[n]}(t)$ of $[n] := \{1, \dots, n\}$ into the clades at time t ; that is, i and j are in the same part if and only if the branchpoint separating the paths to leaves i and j has height $> t$. The consistent growth process serves to define a partition $\Pi(t)$ of

¹⁴Such as a supercritical Galton-Watson tree.

$\mathbb{N} := \{1, 2, \dots\}$ into clades at time t ; explicitly, i and j (with $i, j \in \mathbb{N}$) are in the same part if and only if the branchpoint separating the paths to leaves i and j has height $> t$, in $\text{CTCS}(n)$ for any $n \geq \max(i, j)$. In other words, $\Pi(t)$ is the partition of \mathbb{N} into the clades defined by the infinite tree $\text{CTCS}(\infty)$.

Because each $\text{CTCS}(n)$ is exchangeable, $\Pi(t)$ is an exchangeable random partition of \mathbb{N} , so we can exploit the theory of exchangeable partitions. Denote the clades at time t , that is the parts of $\Pi(t)$, by $\Pi(t)_1, \Pi(t)_2, \dots$, enumerated in order of the least elements. In particular, the clade of leaf 1 is $\Pi(t)_1$. The clades $\Pi(t)_\ell$ are thus subsets of \mathbb{N} , and the clades of $\text{CTCS}(n)$ are the sets $\Pi(t)_\ell \cap [n]$ that are non-empty.

Writing $|\cdot|$ for cardinality, it is easy to show (section 6.11)

Lemma 9 *A.s., all clades $\Pi(t)_\ell$ are infinite, that is $|\Pi(t)_\ell| = \infty$ for every $\ell \geq 1$.*

Write, for $\ell, n \geq 1$,

$$K_{t,\ell}^{(n)} := |\Pi(t)_\ell \cap [n]|; \quad (21)$$

the sequence $K_{t,1}^{(n)}, K_{t,2}^{(n)}, \dots$ is thus the sequence of sizes of the clades in $\text{CTCS}(n)$, extended by 0's to an infinite sequence. Lemma 9 shows that $K_{t,\ell}^{(n)} \rightarrow \infty$ as $n \rightarrow \infty$ for every ℓ . By Kingman's fundamental result [11, Theorem 2.1], the asymptotic proportionate clade sizes, that is the limits

$$P_{t,\ell} := \lim_{n \rightarrow \infty} \frac{K_{t,\ell}^{(n)}}{n}, \quad (22)$$

exist a.s. for every $\ell \geq 1$. Then the random partition $\Pi(t)$ may be constructed (in distribution) from the limits $(P_{t,\ell})_\ell$ by Kingman's paintbox construction, which we state as the following theorem. Note that obviously $P_{t,\ell} \in [0, 1]$, and $\sum_\ell P_{t,\ell} \leq 1$ (by Fatou's lemma); part (i) of the theorem below follows since otherwise a more general version of the paintbox construction would imply that $|\Pi(t)_\ell| = 1$ for some ℓ [11, Proposition 2.8(ii,iii)], which is ruled out by Lemma 9.

Theorem 10 (i) *A.s. each $P_{t,\ell} \in (0, 1)$, and $\sum_\ell P_{t,\ell} = 1$.*

(ii) *Given a realization of $(P_{t,\ell})_\ell$, give each integer $i \in \mathbb{N}$ a random colour ℓ , with probability distribution $(P_{t,\ell})_\ell$, independently for different i . These colours define a random partition of \mathbb{N} , which has the same distribution as $\Pi(t)$.*

Note that the paintbox construction in Theorem 10 starts with the limits $P_{t,\ell}$, but gives as the result $\Pi(t)$ and thus also the partition $\Pi^{[n]}(t)$ for every finite n .

5.3.1 Other proofs?

We believe there should be some “soft” proof of consistency and the exchangeable representation based on the fact [6] that the distribution $q(n, \cdot)$ arises via the first split of n i.i.d. Uniform(0,1) points when the interval is split according to the (improper) density $1/(x(1-x))$. But we have been unable to produce a satisfactory argument along those lines. A more abstract and general approach to such questions was introduced in [31] (see [34] for recent developments) and perhaps can be applied to our model. However, our “concrete” proof allows one to see the explicit inductive construction of the growth process $(\text{CTCS}(n), n \geq 2)$.

5.4 Self-similarity

Consider again the version of $\text{CTCS}(n)$ with all branches extended up to ∞ , see Remark 8. At a fixed height t , the tree $\text{CTCS}(n)$ then consists of one branch for each clade in $\Pi^{[n]}(t)$. We consider the corresponding subtrees of $\text{CTCS}(n)$; that is, we consider the tree $\text{CTCS}(n)$ restricted to times $u \geq t$, which defines a forest $F_t^{(n)}$. The trees in the forest $F_t^{(n)}$ then correspond to the clades at height t in $\text{CTCS}(n)$.

The roots are all at height t , but we may make an obvious time translation so that all roots have height 0.

As n grows, we have the following self-similar behaviour as a consequence of the growth algorithm, see section 6.12.

Theorem 11 *Let $t \geq 0$ be fixed and let n grow from 1 to ∞ . At each increase of n , either one of the trees in $F_t^{(n)}$ gets a new leaf or a new tree consisting only of a root is added to $F_t^{(n)}$; in both cases all other trees in $F_t^{(n)}$ remain unchanged. Moreover, each tree in $F_t^{(n)}$, considered only when it is born or increases in size, grows as a copy of the process $\text{CTCS}(n)$, and different trees grow as independent copies.*

5.5 The subordinator within $\text{CTCS}(\infty)$

The conclusion of the discussion above is that the intuitive idea of a limit continuum tree $\text{CTCS}(\infty)$ can be formalized as the process $(\Pi(t), t \geq 0)$ of partitions of \mathbb{N} , in the spirit of the formalization of *fragmentation processes* in [11]. As with the Brownian continuum random tree context (section 7.3) one can study $\text{CTCS}(\infty)$ as an object in itself, or as a way to prove $n \rightarrow \infty$ limits of aspects of $\text{CTCS}(n)$.

For given n the process $(K_{t,1}^{(n)}, t \geq 0)$ at (21) is the harmonic descent chain (section 3.1) $(X_t^{[n]}, t \geq 0)$ started at state n . We have several times exploited the approximation (4) of this $(K_{t,1}^{(n)}, t \geq 0)$ in terms of the subordinator $(Y_t, 0 \leq t < \infty)$

with Lévy measure ψ_∞ and corresponding σ -finite density f_∞ on $(0, \infty)$ defined in (5), which we for convenience repeat:

$$\psi_\infty[a, \infty) := -\log(1 - e^{-a}); \quad f_\infty(a) := \frac{e^{-a}}{1 - e^{-a}}, \quad 0 < a < \infty. \quad (23)$$

As suggested by (22), this becomes exact in the $n \rightarrow \infty$ limit.

Theorem 12 *Define $Y_t := -\log P_{t,1}$. Then $(Y_t, 0 \leq t < \infty)$ is the subordinator given by (23). Moreover, for $t \geq 0$ and complex s with $\Re s > -1$,*

$$\mathbb{E}[P_{t,1}^s] = \mathbb{E}[e^{-sY_t}] = e^{-t(\psi(s+1) - \psi(1))} \quad (24)$$

where $\psi(z) := \Gamma'(z)/\Gamma(z)$ is the digamma function.

Regarding CTCS(∞) as a tree, the process $(P_{t,1}, t \geq 0)$ is the relative size of the subclade at time t , as one moves a speed 1 down the path to a uniform random leaf on the infinite boundary. We prove Theorem 12 in section 6.13 by calculating moments.

As noted after Theorem 10, for finite n the partition of CTCS(n) into clades at a fixed level t can be also described by the limits $P_{t,\ell}$. Similarly, considering only $\ell = 1$ but all $t \geq 0$ simultaneously, the harmonic descent chain describing the size of the first clade can be reconstructed (in distribution) for any finite n from the process $P_{t,1}$, or equivalently from the subordinator Y_t , as shown by Iksanov [37, 36].

5.6 Proving Theorem 5 via study of CTCS(∞)

Having the exchangeable formalization of CTCS(∞) does not help with our first foundational result (the CLT for leaf-heights: Theorem 2), but (somewhat surprisingly) it does lead to an alternate proof of the second (Theorem 5). This is surprising because convergence of CTCS(n) to CTCS(∞) seems a kind of “global” convergence, whereas the asymptotic fringe is a “local” limit. The central idea of the proof is to define an infinite measure μ on $[0, 1]$ by

$$\mu := \int_0^\infty \mathcal{L}(P_{t,1}) dt. \quad (25)$$

Formula (24) tells us the moments of the measure μ :

$$\int_0^1 x^{s-1} d\mu(x) = \int_0^\infty \mathbb{E}P_{t,1}^{s-1} = \frac{1}{\psi(s) - \psi(1)}, \quad \Re s > 1. \quad (26)$$

So this is the Mellin transform of μ . We do not know how to invert the transform to obtain an explicit formula for μ , but what is relevant to the current proof is the behavior of μ near 0, as follows.

Lemma 13 *Let μ be the infinite measure on $[0, 1)$ having the Mellin transform (26). Then μ is absolutely continuous, with a continuous density $f(x)$ on $(0, 1)$ that satisfies*

$$f(x) = \frac{6}{\pi^2 x} + O(x^{-s_1} + x^{-s_1} |\log x|^{-1}), \quad (27)$$

uniformly for $x \in (0, 1)$, where $s_1 \doteq -0.567$ is the largest negative root of $\psi(s) = \psi(1)$. In particular, for $x \in (0, \frac{1}{2})$ say,

$$f(x) = \frac{6}{\pi^2 x} + O(x^{-s_1}) \text{ as } x \downarrow 0. \quad (28)$$

The (quite technical) proof of the lemma, and the consequent proof of Theorem 5, are given in sections 6.14 and 6.15.

6 Proofs

6.1 Proof of Proposition 1

In CTCS(n) write $(X_n(i, t), i \geq 1)$ for the clade sizes at time t and consider

$$Q_n(t) = \sum_i X_n^2(i, t).$$

Note that, when a size- m clade is split, the effect on sum-of-squares of clade sizes has expectation

$$\sum_{i=1}^{m-1} (m^2 - i^2 - (m-i)^2) q(m, i) = \frac{m}{2h_{m-1}} \sum_{i=1}^{m-1} 2 = \frac{m(m-1)}{h_{m-1}}. \quad (29)$$

If we chose some arbitrary rates $r(m, n)$ for splitting a size- m clade, then

$$\mathbb{E}[Q_n(t) - Q_n(t+dt) | \mathcal{F}_t] = \sum_i r(X_n(i, t), n) \frac{X_n(i, t)(X_n(i, t) - 1)}{h_{X_n(i, t)-1}} dt.$$

So by choosing $r(m, n) = h_{m-1}$ we obtain

$$\mathbb{E}[Q_n(t) - Q_n(t+dt) | \mathcal{F}_t] = (Q_n(t) - n) dt.$$

Because $Q_n(0) = n^2$ we obtain the exact formula

$$\mathbb{E}[Q_n(t)] = n + (n^2 - n)e^{-t}, \quad 0 \leq t < \infty. \quad (30)$$

Now we are studying the height B_n of the branchpoint between the paths to two uniform random distinct leaves of CTCS(n). The conditional probability that both sampled leaves are in clade i at time t equals $\frac{1}{n(n-1)}X_n(i, t)(X_n(i, t) - 1)$. So

$$\begin{aligned}\mathbb{P}(B_n > t) &= \frac{1}{n(n-1)}\mathbb{E}\left[\sum_i X_n(i, t)(X_n(i, t) - 1)\right] \\ &= \frac{1}{n(n-1)}\mathbb{E}[Q_n(t) - n] \\ &= e^{-t} \text{ by (30)}.\end{aligned}$$

6.2 Proof 1 of Theorem 2

6.2.1 The weak law of large numbers

Assume we know the result $\mathbb{E}[D_n] \sim \frac{6}{\pi^2} \log n$, which can be proved by a simple recurrence argument as in section 6.3. Next we need the “weak law”

Lemma 14 $\frac{D_n}{\log n} \rightarrow_p 6/\pi^2$ as $n \rightarrow \infty$.

This follows from the variance estimate (10), which has a more intricate recurrence proof in [8]. Here is our “probability” proof, which spells out the calculation behind the subordinator approximation.

Proof. The process $\log \mathbf{X}$ is itself Markov with transition rates described below. A jump¹⁵ of \mathbf{X} from j to $j-i$ has height $-i$, which corresponds to a jump of $\log \mathbf{X}$ from $\log j$ having height $\log(j-i) - \log j = \log(1 - i/j)$. Define the measure $\tilde{\psi}_j$ on $(-\infty, 0)$ as the measure assigning weight $1/i$ to point $\log(1 - i/j)$, for each $1 \leq i \leq j - 1$. So this measure $\tilde{\psi}_j$ specifies the heights and rates of the downward jumps of $\log \mathbf{X}$ from $\log j$. Writing

$$\tilde{\psi}_j(-\infty, a] = \sum_{i=j(1-e^a)}^{j-1} 1/i \tag{31}$$

shows that there is a $j \rightarrow \infty$ limit measure in the sense

$$\tilde{\psi}_j(-\infty, a] \rightarrow \tilde{\psi}_\infty(-\infty, a] \text{ as } j \rightarrow \infty, \quad -\infty < a < 0 \tag{32}$$

where the limit σ -finite measure $\tilde{\psi}_\infty$ on $(-\infty, 0)$ is the “reflected” version of the measure ψ_∞ on $(0, \infty)$ at (5):

$$\tilde{\psi}_\infty(-\infty, a] := -\log(1 - e^a), \quad \tilde{f}_\infty(a) := \frac{e^a}{1 - e^a}, \quad -\infty < a < 0. \tag{33}$$

¹⁵Note these are *downward* jumps, so take negative values.

In fact we use only a one-sided bound in (32), which we will get by coupling, in two stages. We first define, for $j \geq 2$, a measure $\tilde{\nu}_j$ on $(-\infty, 0)$, whose total mass h_{j-1} is the same as the total mass of $\tilde{\psi}_j$, and where the reflected measures on $(0, \infty)$ satisfy the usual stochastic ordering $\psi_j \preceq \nu_j$ on the line, that is to say

$$\psi_j[0, b] \geq \nu_j[0, b], \quad 0 < b < \infty, \quad j \geq 2.$$

To define $\tilde{\nu}_j$ we simply take the mass $1/i$ of $\tilde{\psi}_j$ at point $\log(1 - i/j)$, for each $1 \leq i \leq j - 1$, and spread the mass over the interval $[\log(1 - (i + 1)/j), \log(1 - i/j)]$ with density proportional to \tilde{f}_∞ . This procedure gives a measure $\tilde{\nu}_j$ with density

$$\tilde{g}_j(u) = b_i \tilde{f}_\infty(u), \quad u \in [\log(1 - (i + 1)/j), \log(1 - i/j)], \quad 1 \leq i \leq j - 1$$

on $-\infty < u < \log(1 - 1/j)$, and $\tilde{g}_j(u) = 0$ on $\log(1 - 1/j) < u < 0$, where

$$b_i := \frac{1}{i(\log(i + 1) - \log i)}, \quad i \geq 1.$$

Clearly we have the stochastic ordering $\psi_j \preceq \nu_j$ of the reflected measures. Define a kernel density, for $a > 0$ and $u < 0$,

$$\kappa(a, u) := \tilde{g}_j(u) \text{ on } \log(j - 1) < a \leq \log j, \quad j \geq 2;$$

let also $\kappa(a, u) = 0$ for $a \leq 0$. Now write $(Z_t^{(n)}, t \geq 0)$ for the decreasing Markov process on $(0, \infty)$, starting at $Z_0^{(n)} = \log n$, for which the heights u and rates κ of the downward jumps from a are given by $\kappa(a, u)$. The stochastic ordering relation $\psi_j \preceq \nu_j$ between the driving measures of the processes $\log \mathbf{X}^{(n)}$ and $\mathbf{Z}^{(n)}$, together with the fact that $\log \mathbf{X}^{(n)}$ is stochastically monotone, imply that we can couple the two processes so that

$$\log X_t^{(n)} \geq Z_t^{(n)}. \tag{34}$$

Now fix small $\varepsilon > 0$ and define a density $\tilde{f}_\infty^\varepsilon$ on $(-\infty, 0)$ by

$$\tilde{f}_\infty^\varepsilon(u) = 2\tilde{f}_\infty(u), \quad -\varepsilon < u < 0 \tag{35}$$

$$= (1 + \varepsilon)\tilde{f}_\infty(u), \quad -\infty < u \leq -\varepsilon. \tag{36}$$

Because $2 > b_i \downarrow 1$ as $i \rightarrow \infty$, there exists $j(\varepsilon)$ such that

$$\tilde{g}_j \leq \tilde{f}_\infty^\varepsilon \text{ for all } j > j(\varepsilon)$$

and therefore

$$\kappa(a, u) \leq \tilde{f}_\infty^\varepsilon(u), \quad a \geq \log j(\varepsilon). \tag{37}$$

Now consider the subordinator \mathbf{Y}^ε with Lévy density $f_\infty^\varepsilon(u) := \tilde{f}_\infty^\varepsilon(-u)$ on $(0, \infty)$. The inequality (37) implies that we can couple $\mathbf{Z}^{(n)}$ and \mathbf{Y}^ε as

$$Z_t^{(n)} \geq \log n - Y_t^\varepsilon \text{ while } \log n - Y_t^\varepsilon \geq j(\varepsilon). \quad (38)$$

Now the strong law of large numbers for \mathbf{Y}^ε is

$$t^{-1}Y_t^\varepsilon \rightarrow \rho^\varepsilon := \int_0^\infty u f_\infty^\varepsilon(u) du.$$

Combining this with (34, 38) and noting that $\rho^\varepsilon \downarrow \rho = \pi^2/6$ by (7), it is straightforward to deduce that, for the coupling used here,

$$\liminf_n D_n / \log n \geq 6/\pi^2 \text{ a.s.}$$

Together with the upper bound on $\mathbb{E}[D_n]$ from Theorem 16, this implies $D_n / \log n \rightarrow_p 6/\pi^2$. ■

6.2.2 The Gaussian limit

Recall that D_n is the time that our size-biased chain $(X_t^{(n)})$ is absorbed at 1. Recalling (4) and (6), the first-order approximation for $(X_t^{(n)})$ is

$$\log X_t^{(n)} \approx \log n - \rho t, \quad 0 \leq t \leq \rho^{-1} \log n$$

where $\rho = \mu^{-1} = \pi^2/6$. To study the second-order structure, we standardize as follows. Subtract the first order approximation, divide by $\sqrt{\log n}$ (the desired order of the s.d.) and speed up by $\log n$ (the order of $\mathbb{E}[D_n]$). So the standardized process is

$$\tilde{S}_s^{(n)} := \frac{\log X_{s \log n}^{(n)} - \log n + \rho s \log n}{\sqrt{\log n}}, \quad 0 \leq s \leq \rho^{-1} \quad (39)$$

and essentially we want to show this converges in distribution to Brownian motion.

The first step is that the rates (3) determine the infinitesimal drift rate $a(j)$ and the variance rate $b(j)$ of $\log X_t$ when $X_t = j$, as follows.

$$a(j) := \sum_{1 \leq i \leq j-1} \frac{\log i - \log j}{j - i}; \quad b(j) := \sum_{1 \leq i \leq j-1} \frac{(\log i - \log j)^2}{j - i}. \quad (40)$$

Approximating the sums by integrals,

$$a(j) \rightarrow -\rho \text{ and } b(j) \rightarrow \int_0^1 \frac{\log^2 y}{1 - y} dy =: \sigma^2 = 2\zeta(3) \text{ as } j \rightarrow \infty. \quad (41)$$

We will need a bound on the former rate of convergence, but we do not need a bound for $b(j)$. Applying Euler's summation formula¹⁶ (Graham, Knuth, and Patashnik [28], (9.78)) for a smooth function f ,

$$\sum_{a \leq i < b} f(i) = \int_a^b f(x) dx - \frac{1}{2}f(x)\Big|_a^b + \frac{1}{12}f'(x)\Big|_a^b + O\left(\int_a^b |f''(x)| dx\right),$$

to $f_j(x) = \frac{\log x - \log j}{j-x}$, one can show

$$|a(j) + \rho| = O(j^{-1} \log j). \quad (42)$$

To start a proof of convergence, we need to stop the process before $X_t = O(1)$, so take the stopping time

$$T_n := \min\{t : \log X_t^{(n)} \leq \log^{1/3} n\}$$

and replace (39) by the stopped process

$$S_s^{(n)} := \frac{\log X_{\min(s \log n, T_n)}^{(n)} - \log n + \rho \min(s \log n, T_n)}{\sqrt{\log n}}, \quad 0 \leq s < \infty.$$

The central issue is to prove the following. Write $(B_s, 0 \leq s < \infty)$ for standard Brownian motion. Recall $\mu = \rho^{-1} = 6/\pi^2$ and $\sigma^2 = 2\zeta(3)$.

Proposition 15 $(S_s^{(n)}, 0 \leq s < \infty) \rightarrow_d (\sigma B_{\min(s, \mu)}, 0 \leq s < \infty)$ in the usual Skorokhod topology.

Granted Proposition 15, we proceed as follows. Clearly $T_n \leq D_n$ and from $\mathbb{E}[D_m] \sim \mu \log m$ we have

$$\mathbb{E}[D_n - T_n] = O(\log^{1/3} n). \quad (43)$$

Combining this with Lemma 14, that $D_n/\log n \rightarrow_p \mu$, we have

$$T_n/\log n \rightarrow_p \mu. \quad (44)$$

From Proposition 15 at $s = T_n/\log n$ we have

$$S_{T_n/\log n}^{(n)} \rightarrow_d \sigma B_\mu =_d \text{Normal}(0, \mu\sigma^2)$$

and then from the definition of $S_s^{(n)}$

$$\frac{T_n - \mu \log n}{\mu \sqrt{\log n}} \rightarrow_d \text{Normal}(0, \mu\sigma^2).$$

¹⁶Variants of this formula play a central role in the precise estimates in [8].

Using (43) again, we can replace T_n by D_n , and then rewrite as

$$\frac{D_n - \mu \log n}{\sqrt{\log n}} \rightarrow_d \text{Normal}(0, \mu^3 \sigma^2)$$

as in Theorem 2.

Proof of Proposition 15. Recall the infinitesimal rates $a(j)$ and $b(j)$ at (41). Consider the Doob-Meyer decomposition $S^{(n)} = A^{(n)} + M^{(n)}$ in which $A^{(n)}$ is a continuous process and $M^{(n)}$ is a martingale. In this decomposition $S_0^{(n)} = A_0^{(n)} = M_0^{(n)} = 0$ and $A_t^{(n)} = \int_0^t dA_s^{(n)}$ and one readily sees that

$$dA_s^{(n)} = (\log^{1/2} n) (a(X_{s \log n}^{(n)}) + \mu^{-1}) ds.$$

Here and in what follows we need only consider $s < T_n / \log n$.

The increasing process $\langle M^{(n)} \rangle_t$ associated with $M^{(n)}$, that is the continuous component of the Doob-Meyer decomposition of $(M^{(n)})^2$, is

$$d \langle M^{(n)} \rangle_s = b(X_{s \log n}^{(n)}) ds. \quad (45)$$

To prove Proposition 15, it will suffice to prove

- (i) $A^{(n)}$ converges to the zero process
- (ii) $M^{(n)}$ converges to the stopped Brownian motion process $(\sigma B_{\min(s, \mu)}, 0 \leq s < \infty)$.

For (i) it is enough to show

$$(\log^{1/2} n) \int_0^{T_n / \log n} |a(X_{s \log n}^{(n)}) + \mu^{-1}| ds \rightarrow_p 0 \text{ as } n \rightarrow \infty \quad (46)$$

and (because $X_{s \log n}^{(n)} \geq \exp(\log^{1/3} n)$ on the interval of integration) the bound $|a(j) + \mu^{-1}| = O(j^{-1} \log j)$ from (42) is, together with (44), more than sufficient to prove (46).

By one version of the classical martingale CLT (Helland [33] Theorem 5.1(a)), to prove (ii) it suffices to show that for each $t < \mu$

$$\langle M^{(n)} \rangle_t \rightarrow_p \sigma^2 t \quad (47)$$

$$\rho^\varepsilon [M^{(n)}]_t := \sum_{u \leq t} |\Delta M^{(n)}(u)|^2 \mathbf{1}_{\{|\Delta M^{(n)}(u)| > \varepsilon\}} \rightarrow_{L^1} 0 \quad (48)$$

where the sum is over jumps $\Delta M^{(n)}(u) := M^{(n)}(u) - M^{(n)}(u-)$. In fact, [33, Theorem 5.1(a)] uses instead of (48) the assumption that the compensator of $\rho^\varepsilon [M^{(n)}]_t$

tends to 0 in probability for each t ; this is a weaker assumption, since an increasing process and its compensator have the same expectation, and thus (48) implies convergence of the compensator to 0 in L^1 and thus in probability.

Now (47) is immediate from (41) and (45). To prove (48), we require only very crude bounds. The jumps of $M^{(n)}$ are the jumps of $S^{(n)}$ which are the jumps of $(\log^{-1/2} n) \log X^{(n)}$. So $0 > \Delta M^{(n)}(u) \geq -\log^{1/2} n$, and it suffices to show that for fixed $\varepsilon > 0$, the number of large jumps satisfies

$$(\log n) \mathbb{E}[|\{u \leq T_n / \log n : \Delta M^{(n)}(u) \leq -\varepsilon\}|] \rightarrow 0.$$

In other words, it suffices to show

$$(\log n) \mathbb{E}[|\{u \leq T_n : \log X_{u-}^{(n)} - \log X_u^{(n)} \geq \varepsilon \log^{1/2} n\}|] \rightarrow 0. \quad (49)$$

Now from the transition rates (3) for X_t , we have

for $1 \leq i \leq j/2$, the rate of jumps from j to some $k \leq i$ equals $\sum_{k=1}^i 1/(j-k) \leq 2i/j$.

The jumps in (49) are from some state j to a state below i where $i/j = \exp(-\varepsilon \log^{1/2} n)$, and so (for large n) occur at rate at most $\alpha_n := 2 \exp(-\varepsilon \log^{1/2} n)$. So the expectation in (49) is at most $\mathbb{E}[T_n] \alpha_n \sim (\mu \log n) \alpha_n$. Now $(\mu \log^2 n) \alpha_n \rightarrow 0$ as required to establish (49).

6.3 An illustration of analysis of recursions

Here we illustrate the methodology behind Theorem 3. We will copy the first steps of the proof in [8] of our (9) to get the weaker result below. The proof uses only the elementary recurrence for $t_n := \mathbb{E}D_n$:

$$t_n = \frac{1}{h_{n-1}} \left(1 + \sum_{i=1}^{n-1} \frac{t_i}{n-i} \right) \quad (50)$$

with $t_1 = 0$. One can see the first order result $\mathbb{E}[D_n] \sim \frac{6}{\pi^2} \log n$ heuristically by plugging $c \log n$ into the recursion and taking the natural first-order approximation to the right side; the constant c would emerge as the inverse of the constant

$$\int_0^1 \frac{\log(1/x)}{1-x} dx = \zeta(2) = \frac{\pi^2}{6} \quad (51)$$

and indeed this is how it emerges in the proof below.

Proposition 16

$$\mathbb{E}[D_n] = \frac{6}{\pi^2} \log n + O(\log \log n) \text{ as } n \rightarrow \infty.$$

Proof. The proof involves three steps.

Step 1. We shall prove

$$\mathbb{E}[D_n] \geq \frac{6}{\pi^2} \log n, \quad n \geq 1. \quad (52)$$

Setting $\tau_n = A \log n$ for $A = 6/\pi^2$, it suffices to show

$$\frac{1}{h_{n-1}} \left(1 + \sum_{k=1}^{n-1} \frac{\tau_k}{n-k} \right) \geq \tau_n, \quad n \geq 2, \quad (53)$$

because then, by (50) and induction on n , $\mathbb{E}[D_n] \geq \tau_n$ for all $n \geq 1$, establishing (52). We compute

$$\begin{aligned} \frac{1}{h_{n-1}} \left(1 + \sum_{k=1}^{n-1} \frac{\tau_k}{n-k} \right) &= \frac{1}{h_{n-1}} \left(1 + \sum_{k=1}^{n-1} \frac{A \log k}{n-k} \right) \\ &= \frac{1}{h_{n-1}} \left(1 + A(\log n)h_{n-1} + A \sum_{k=1}^{n-1} \frac{\log(k/n)}{n(1-k/n)} \right) \\ &= \tau_n + \frac{1}{h_{n-1}} \left(1 + A \sum_{k=1}^{n-1} \frac{\log(k/n)}{n(1-k/n)} \right) \\ &\geq \tau_n + \frac{1}{h_{n-1}} \left(1 - A \int_0^1 \frac{\log(1/x)}{1-x} dx \right). \end{aligned}$$

The inequality holds because the integrand is positive and decreasing. So by (51), the choice $A = 6/\pi^2$ establishes (53).

Step 2. Let us prove

$$\mathbb{E}[D_n] \leq f(n) \quad (54)$$

where

$$f(x) := \begin{cases} x - 1, & x \leq 2, \\ 1 + \log(x - 1), & x \geq 2. \end{cases} \quad (55)$$

This is true for $n = 1$ since $\mathbb{E}[D_1] = 0$. So, similarly to (53), it is enough to show that $f(n)$ satisfies

$$f(n) \geq \frac{1}{h_{n-1}} \left(1 + \sum_{i=1}^{n-1} \frac{f(i)}{n-i} \right), \quad n \geq 2. \quad (56)$$

Since $f(x)$ is *concave*, we have

$$\begin{aligned} \frac{1}{h_{n-1}} \left(1 + \sum_{i=1}^{n-1} \frac{f(i)}{n-i} \right) &\leq \frac{1}{h_{n-1}} + f \left(\frac{1}{h_{n-1}} \sum_{i=1}^{n-1} \frac{i}{n-i} \right) \\ &= \frac{1}{h_{n-1}} + f \left(n - \frac{n-1}{h_{n-1}} \right) \leq \frac{1}{h_{n-1}} + f(n) - f'(n) \left(\frac{n-1}{h_{n-1}} \right), \end{aligned}$$

which is exactly $f(n)$, since $f'(x) = \frac{1}{x-1}$ for $x \geq 2$.

Step 3. Let $n_0 \geq 2$, and

$$A = A(n_0) := \left(\int_{1/n_0}^1 \frac{\log(1/x)}{1-x} dx \right)^{-1}, \quad B = B(n_0) := n_0^{\frac{2}{A \log 2} - 1}.$$

We shall prove

$$\mathbb{E}[D_n] \leq A \log(nB), \quad n \geq 2. \quad (57)$$

This inequality certainly holds for $n \leq n_0$, because, by (54), for those n

$$\mathbb{E}[D_n] \leq \frac{2}{\log 2} \log n = A \log n \cdot \frac{2}{A \log 2} = A \log \left(n^{\frac{2}{A \log 2}} \right) \leq A \log(nB).$$

Therefore it suffices to show that $\tau_n := A \log(nB)$ satisfies

$$\frac{1}{h_{n-1}} \left(1 + \sum_{i=1}^{n-1} \frac{\tau_i}{n-i} \right) \leq \tau_n, \quad n > n_0. \quad (58)$$

Plugging $\tau_i = \tau_n - A \log(n/i)$ into the left side of (58), we rewrite it as follows, cf. Step 1:

$$\begin{aligned} \frac{1}{h_{n-1}} \left(1 + \sum_{i=1}^{n-1} \frac{\tau_i}{n-i} \right) &= \frac{1}{h_{n-1}} \left(1 + \tau_n \cdot h_{n-1} - A \sum_{i=1}^{n-1} \frac{\log(n/i)}{n(1-i/n)} \right) \\ &\leq \tau_n + \frac{1}{h_{n-1}} \left(1 - A \int_{1/n}^1 \frac{\log(1/x)}{1-x} dx \right) \\ &\leq \tau_n + \frac{1}{h_{n-1}} \left(1 - A \int_{1/n_0}^1 \frac{\log(1/x)}{1-x} dx \right) \\ &= \tau_n. \end{aligned}$$

This establishes (58) and thus (57).

Step 4. Note that $A(n_0) \leq \frac{6}{\pi^2} + O(\frac{\log n_0}{n_0})$ and $\log B(n_0) = O(\log n_0)$. So choosing $n_0 = \lceil \log n \rceil$ we have

$$A(n_0) \log(nB(n_0)) \leq \left(\frac{6}{\pi^2} + O\left(\frac{\log \log n}{\log n}\right) \right) (\log n + O(\log \log n)).$$

So (57) establishes the upper bound in Theorem 16, and (52) establishes the lower bound. ■

Discussion. The seemingly naive idea is to replace a recurrence equality by a recurrence *inequality* for which an explicit solution can be found and then to use it to upper bound the solution of the recurrence *equality*. And one can use probabilistic heuristics to guess the asymptotic behavior, and then check that a slightly larger function satisfies the recurrence inequality.

6.4 Bounds for the tree height

To study the maximum leaf height D_n^* , we will need a tail bound on D_n .

Lemma 17 $\mathbb{P}(D_n > t) \leq (n-1)e^{-t}$, $0 \leq t < \infty$.

Proof. Write $(X_t \equiv X_t^{(n)}, 0 \leq t < \infty)$ for the HD chain started at $X_0 = n$, so $D_n = \inf\{t : X_t = 1\}$. From the transition rates,

$$\mathbb{E}(dX_t | X_t = j) = - \sum_{i=1}^{j-1} (j-i)/(j-i) dt = -(j-1)dt \text{ on } \{X_t \geq 2\}.$$

So setting $Y_t := X_t - 1$ we have $Y_0 = n-1$ and

$$\mathbb{E}[dY_t | \mathcal{F}_t] = -Y_t dt, \quad 0 \leq t < \infty.$$

So

$$\mathbb{E}[Y_t] = (n-1)e^{-t}$$

and then

$$\mathbb{P}(D_n > t) = \mathbb{P}(Y \geq 1) \leq (n-1)e^{-t}.$$

■

Now from Boole's inequality and Lemma 17

$$\mathbb{P}(D_n^* > t) \leq n\mathbb{P}(D_n > t) \leq n(n-1)e^{-t}$$

and so

Corollary 18

$$\begin{aligned} \mathbb{P}(D_n^* > (2 + \varepsilon) \log n) &\rightarrow 0 \text{ for all } \varepsilon > 0 \\ \mathbb{E}[D_n^*] &\leq \int_0^\infty \min(1, n(n-1)e^{-t}) dt \leq 1 + 2 \log n. \end{aligned}$$

6.5 The conjecture for maximum leaf height

One aspect where there may be a substantial difference between the discrete and continuous time models concerns the tree height. We will discuss the DTCS(n) case in section 6.6. For CTCS(n), recall the CLT:

$$\frac{D_n - \mu \log n}{\sqrt{\log n}} \rightarrow_d \text{Normal}(0, \mu^3 \sigma^2) \text{ as } n \rightarrow \infty$$

where $\mu := 1/\zeta(2) = 6/\pi^2 = 0.6079\dots$; $\sigma^2 := 2\zeta(3) = 2.4041\dots$. We conjectured at (13)

$$D_n^* \sim c \log n \text{ in probability, where } c := 1 + \mu + \mu^3 \sigma^2 / 2 = 1.878\dots$$

A naive starting argument would be to believe that D_n^* behaves as the maximum of n i.i.d. samples from the approximating Normal distribution, which would give

$$D_n^* \approx \mu \log n + \sqrt{2 \log n} \times \sqrt{\mu^3 \sigma^2 \log n} = (1 + 2^{1/2} \sigma \mu^{3/2}) \log n = 1.65\dots \log n. \quad (59)$$

But (59) is in fact not the right way to study D_n^* , because of the “fringe” behavior in the continuous model. Figure 3 gives a hint about the issue, which is that there are some unusually long terminal edges to a pair of leaves. The CTCS(n) tree has order n terminal edges to a pair of leaves; in the heuristics below we take as this as n for simplicity (this should only affect the estimate of D_n^* by $\pm O(1)$). These n edges have i.i.d. Exponential(1) distribution, and the (asymptotic) structure of the largest of these n lengths is well-known: the lengths in decreasing order are

$$(\log n + \xi_1, \log n + \xi_2, \log n + \xi_3, \dots)$$

where $\infty > \xi_1 > \xi_2 > \xi_3 > \dots > -\infty$ are the largest points of the Poisson point process on \mathbb{R} with rate e^{-x} , so that ξ_1 has the standard Gumbel distribution

$$\mathbb{P}(\xi_1 \leq x) = \exp(-e^{-x}), \quad -\infty < x < \infty.$$

By imagining that the longest such edge is attached to the tree at the typical leaf depth D_n , and using the Normal limit for the random leaf heights D_n , we assert a lower bound

$$\mathbb{P}(D_n^* \leq (\mu + 1) \log n - \omega_n \sqrt{\log n}) \rightarrow 0 \text{ for any } \omega_n \rightarrow \infty.$$

which one could certainly make rigorous. However, we conjecture that we get the right behavior for D_n^* by maximizing over all the $o(n)$ longest fringe edges. Imagine that each of these longest fringe edges is attached to the tree at independent depths D_n . So

$$D_n^* \approx (\mu + 1) \log n + H_n$$

$$H_n := \max_i (\xi_i + \nu_i)$$

for (ξ_i) as above and (ν_i) i.i.d. Normal $(0, \alpha_n^2)$, with $\alpha_n^2 = \mu^3 \sigma^2 \log n$ in the notation of the Normal limit for D_n .

To analyze H_n , write $\bar{\Phi}_n(\cdot)$ for the tail distribution function of Normal $(0, \alpha_n^2)$. Because the pairs (ξ_i, ν_i) form a Poisson process we have

$$\begin{aligned} -\log \mathbb{P}(H_n \leq y) &= \int_{-\infty}^{\infty} e^{-x} \bar{\Phi}_n(y-x) dx & (60) \\ &= e^{-y} \int_{-\infty}^{\infty} e^{y-x} \bar{\Phi}\left(\frac{y-x}{\alpha_n}\right) dx \\ &= e^{-y} \alpha_n \int_{-\infty}^{\infty} e^{\alpha_n u} \bar{\Phi}(u) du \end{aligned}$$

where $\bar{\Phi}$ refers to the standard Normal distribution, and $\phi(\cdot)$ below is its density. The integrand above is maximized for u around α_n , so setting $v = u - \alpha_n$ and using $\bar{\Phi}(z) \sim \phi(z)/z$ as $z \rightarrow \infty$,

$$\begin{aligned} &\approx e^{-y} \alpha_n \frac{1}{\sqrt{2\pi}} \int_{-\infty}^{\infty} \exp(\alpha_n(v + \alpha_n)) \exp(-(v + \alpha_n)^2/2) \frac{1}{v + \alpha_n} dv \\ &\approx e^{-y} \frac{1}{\sqrt{2\pi}} \int_{-\infty}^{\infty} \exp(-v^2/2 + \alpha_n^2/2) dv \\ &= e^{-y} e^{\alpha_n^2/2}. \end{aligned}$$

Putting all this together

$$-\log \mathbb{P}(H_n \leq y + \alpha_n^2/2) \approx e^{-y}$$

and the final conclusion is

$$D_n^* \approx c \log n + \xi; \quad c := 1 + \mu + \mu^3 \sigma^2 / 2 = 1.878\dots$$

where ξ has standard Gumbel distribution.

Now this outline is too crude to believe that the $+\xi$ term above is correct, but this value of c seems plausible. Here is one “reality check” for the argument/calculation above. Look back at the first integral (60): for given y , the relevant values of x are around $y - \alpha_n^2$. The relevant values of y are around $\alpha_n^2/2$, so overall the relevant values of x are around $-\alpha_n^2/2$. This corresponds to the ν_i around position $-\alpha_n^2/2$, and the number of such edges is around $\exp(\alpha_n^2/2) \approx n^{0.27}$. So one implicit assumption was

If we pick $n^{0.27}$ random leaves from $\text{CTCS}(n)$, then the distribution of their maximum height is essentially the same as $n^{0.27}$ picks from the corresponding Normal distribution.

Is this plausible? As proved in [8], the correlation between the heights of two typical leaves tends to zero as $n \rightarrow \infty$.¹⁷ But now one should pay attention to the labels $\{1, 2, \dots, n\}$ in the interval-splitting representation; roughly, we would need to bound the association between the tail distributions of heights of leaf i and leaf $i + n^{0.73}$.

6.6 The height of $\text{DTCS}(n)$

In this article we have focussed on the continuous model $\text{CTCS}(n)$ rather than the discrete model $\text{DTCS}(n)$, motivated by the consistency property of the continuous model. As mentioned in section 3.3, for the precise asymptotics of leaf heights in $\text{CTCS}(n)$ in Theorem 3 there are parallel results in [8] for $\text{DTCS}(n)$. An apparent difference between the two models arises when we study the tree height, which (as noted in section 6.5) in $\text{CTCS}(n)$ is affected by the extremes of the terminal edge lengths, which cannot happen for $\text{DTCS}(n)$. We remark that section 7.1 contains a specific context where the discrete tree height is relevant.

Write L_n^* and L_n for the tree height and the height of a random leaf in $\text{DTCS}(n)$. Recall (11) that $\mathbb{E}[L_n] \sim 3\pi^{-2} \log^2 n$. Proved in [8] is an analog of Proposition 4:

$$\mathbb{P}(L_n^* > \beta \log^2 n) \rightarrow 0 \text{ for } \beta > \beta_0 \doteq 0.93.$$

Analogous to Open Problem 1 we conjecture

Open Problem 7 *Show that $L_n^* \sim c \log n$ in probability, and identify the constant c .*

One could also¹⁸ consider the length L_n^+ of the path from the root that is chosen via the natural greedy algorithm, taking the larger sub-clade at each split. Numerics suggest that $\mathbb{E}[L_n^+ - L_n]$ grows slightly faster than $(\log n) \cdot (\log \log n)$. This suggests that the limit constant c may in fact be the lower bound $3\pi^{-2}$ given by (11).

¹⁷Because the common part of the two paths is $O(1)$, and the parts after branching are independent, conditioned on the splitting time and the sizes of the two branches there. Note that the arXiv version 3 preprint of [8] mistakenly asserts that the limit correlation is non-zero; a correct argument will appear in version 4.

¹⁸This idea is mentioned in [6] but there is a foolish calculus error leading to an incorrect conclusion.

6.7 Length of CTCS(n)

We re-state Proposition 6:

$$\lim_n n^{-1} \mathbb{E}[\Lambda_n] = \frac{6}{\pi^2}$$

where Λ_n is the length of CTCS(n).

Proof. We need to justify the implicit interchange of limits in the argument in section 4.5. Of course Fatou's lemma and (19)–(20) tell us that

$$\liminf n^{-1} \mathbb{E}[\Lambda_n] \geq 6/\pi^2. \quad (61)$$

We will use several pieces of previous theory. In the context of the consistency property, Figure 10 illustrated the “delete and prune” operation. Deletion of each possible type of leaf (a, b, c in the Figure) decreases the number of edges by 1, but only (b) and (c) reduce the length of the tree. In fact in the inductive construction, essentially the inverse of the “cut and prune” operation, at each step the total length is either unchanged or is increased by an Exponential(1) amount. So in particular

$$\mathbb{E}[\Lambda_n] \leq \mathbb{E}[\Lambda_{n+1}] \leq \mathbb{E}[\Lambda_n] + 1. \quad (62)$$

We need a fact from the analysis of the HD chain in [7]. For $n \geq 2$

$$a(i) = \sum_{j=i}^n \hat{b}_n(j) a(j, i), \quad i \leq n \quad (63)$$

where, with $q^*(m, j)$ from (2),

$$\hat{b}_n(j) := \sum_{m>n} a(m) q^*(m, j), \quad 1 \leq j \leq n,$$

is the overshoot distribution, that is the distribution of the state where the chain enters $[[1, n]]$. Dividing (63) by ih_{i-1} and summing over i

$$\sum_{i=2}^n \sum_{j=i}^n \hat{b}_n(j) \frac{a(j, i)}{ih_{i-1}} = \sum_{i=2}^n \frac{a(i)}{ih_{i-1}}$$

and then from (19) for $\mathbb{E}[\Lambda_j]$ and the summation at (20)

$$\sum_{j=2}^n \hat{b}_n(j) \frac{\mathbb{E}[\Lambda_j]}{j} = \frac{6}{\pi^2} \left(1 - \frac{1}{n}\right). \quad (64)$$

As a final ingredient, the overshoot distribution $\hat{b}_n := \text{dist}(V_n)$ has a scaling limit¹⁹ $n^{-1}V_n \rightarrow_d V$ where V has support $[0, 1]$.

¹⁹Explicitly, V has density $f_V(v) = 6\pi^{-2} \int_1^\infty \frac{1}{x(x-v)} dx = 6\pi^{-2} \frac{-\log(1-v)}{v}$.

To complete a proof by contradiction, suppose

$$\limsup n^{-1}\mathbb{E}[\Lambda_n] > 6/\pi^2.$$

Then, using (62), there exist $\varepsilon > 0$ and infinitely many n_0 such that $j^{-1}\mathbb{E}[\Lambda_j] \geq 6/\pi^2 + \varepsilon$ for all $n_0(1 - \varepsilon) \leq j \leq n_0$. But this and (61) and the scaling limit for \hat{b}_n imply

$$\limsup_n \sum_{j=2}^n \hat{b}_n(j) \frac{\mathbb{E}[\Lambda_j]}{j} \geq \frac{6}{\pi^2} + \varepsilon \mathbb{P}(1 - \varepsilon < V < 1) > \frac{6}{\pi^2}$$

contradicting (64). ■

6.8 Proof of the consistency property

Recall the statement of Theorem 7:

The operation “delete and prune leaf $n + 1$ from $\text{CTCS}(n + 1)$ ” gives a tree distributed as $\text{CTCS}(n)$.

The argument below uses unlabelled leaves. In the context of Theorem 7 we then apply a uniform random permutation to label leaves as $1, \dots, n$, so that “delete leaf n ” is equivalent to “delete a uniform random leaf”.

We work with the pruned representation of a tree (see Figure 11), so we should be careful about what it means for two trees to be the same or different. First, the left/right distinction matters; switching gives a different tree (because edge-lengths in our model are independent Exponentials, different edges cannot have the same length), and switching a side-bud to the other side gives a different tree. But buds are unlabelled, so switching the two buds in a bud-pair gives the same tree.

Consider a pair of trees $(\mathbf{t}_n, \mathbf{t}_{n+1})$ with n and $n + 1$ leaves, in which \mathbf{t}_n can be obtained from \mathbf{t}_{n+1} via the “delete a bud and prune” operation in Figure 10. So \mathbf{t}_{n+1} arises by adding a new bud to \mathbf{t}_n , which can happen in one of three qualitative ways, illustrated in Figure 11. The addition is either what we will call a *side-bud extension* (case **a** in Figure 11) in which a side-bud is attached at the interior of some existing edge, or a *branch extension* (case **b**) in which one bud of a terminal pair grows into a new branch to a terminal pair of buds, or a *side-bud extension* (case **c**) in which a side-bud grows into a new branch with two terminal buds.

We will do explicit calculations for $(\text{CTCS}(3), \text{CTCS}(4))$ in the following section. This enables one to guess the inductive algorithm, which we state and verify for general n in section 6.8.2.

6.8.1 A starting step

The distribution of $\text{CTCS}(n)$ is specified by the shape of the tree and the probability density of the edge-lengths. For $n = 3$ there are only two possible shapes, as \mathbf{t} in

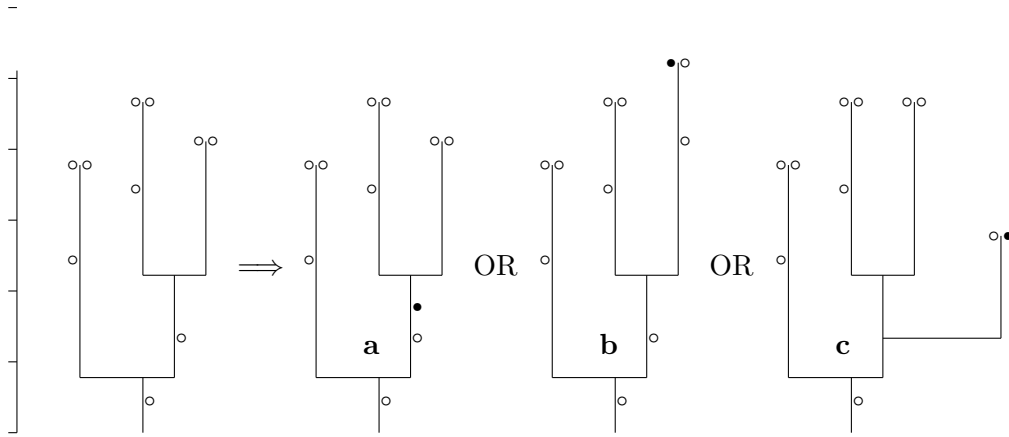


Figure 11: Possible transitions from CTCS(10) to CTCS(11): the added bud is \bullet .

Figure 12 and as its “reflection” with the side-bud on the left instead of the right. There are two edge-lengths (a, b) . Clearly the density of CTCS(3) is

$$f(\mathbf{t}; a, b) = \frac{1}{2} h_2 e^{-h_2 a} \cdot e^{-b}; \quad 0 < a, b < \infty \quad (65)$$

and the probability of \mathbf{t} is $1/2$. There are 7 shapes of CTCS(4) that are consistent with this \mathbf{t} , shown as $\mathbf{t}_1, \mathbf{t}_2, \mathbf{t}_3, \mathbf{t}_4$ in Figure 12, together with the “reflected” forms of \mathbf{t}_1 and \mathbf{t}_3 and \mathbf{t}_4 (the added side-bud involves the other side; drawn as $\hat{\mathbf{t}}_1, \hat{\mathbf{t}}_3, \hat{\mathbf{t}}_4$) which will be accounted for as $q(\cdot, \cdot) + q(\cdot, \cdot)$ terms in the calculation below.²⁰ The densities of these shapes involve 3 edge-lengths (a, b, c) , calculated below as $f_i^+(a, b, c)$. We also calculate the marginals $f_i(a, b) = \int f_i^+(a, b, c) dc$. The consistency assertion that we wish to verify is the assertion, for $f = f(\mathbf{t}; \cdot, \cdot)$ as at (65),

$$f \stackrel{?}{=} \frac{1}{4} f_1 + \frac{2}{4} f_2 + \frac{1}{4} f_3 + \frac{2}{4} f_4 \quad (66)$$

where the fractions denote the probability that deleting a random bud gives \mathbf{t} with

²⁰That is, f_1^+ is the density of \mathbf{t}_1 plus the density of $\hat{\mathbf{t}}_1$.

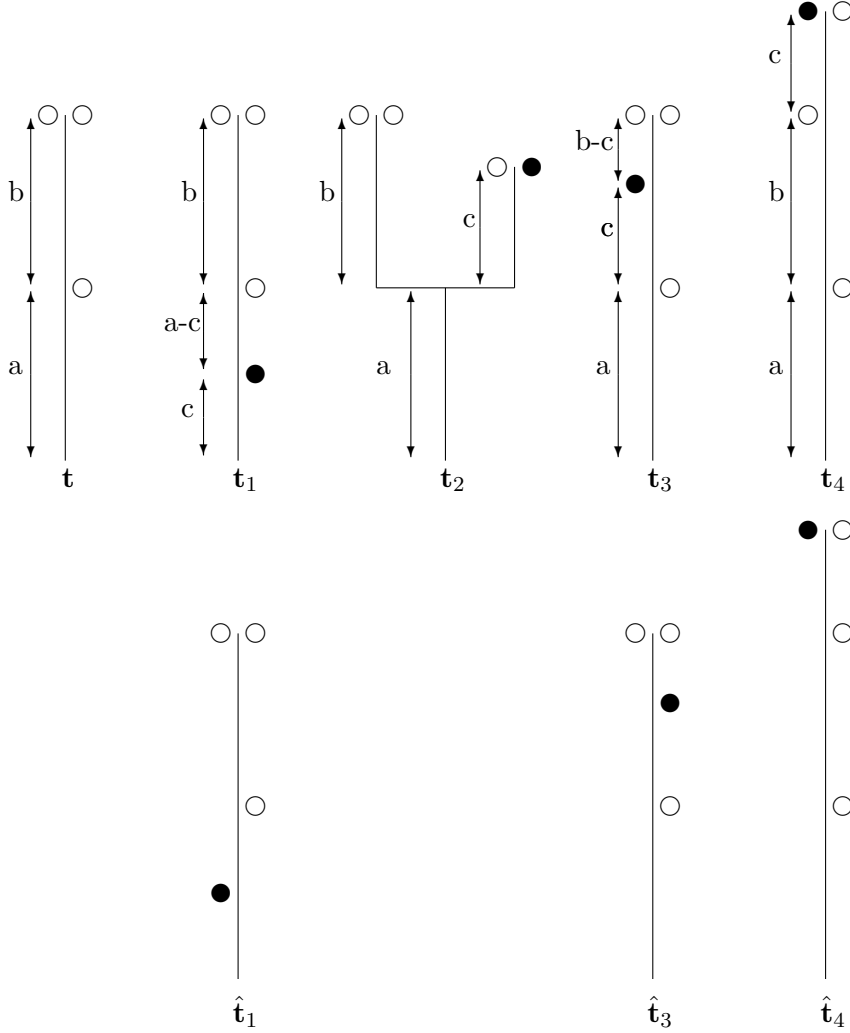


Figure 12: The possible transitions from \mathbf{t} : the added bud is \bullet .

the given edge-lengths (a, b) . From the definition of CTCS(4) we can calculate

$$\begin{aligned}
f_1^+(a, b, c) &= (q(4, 1) + q(4, 3)) \cdot h_3 e^{-h_3 c} \cdot q(3, 2) \cdot h_2 e^{-h_2(a-c)} \cdot e^{-b} \\
f_1(a, b) &= (q(4, 1) + q(4, 3)) \cdot h_3 \cdot 3(1 - e^{-a/3}) \cdot q(3, 2) \cdot h_2 e^{-h_2 a} \cdot e^{-b} \\
&= 3(e^{-h_2 a} - e^{-h_3 a}) \cdot e^{-b} \\
f_2^+(a, b, c) &= q(4, 2) \cdot h_3 e^{-h_3 a} \cdot e^{-b} e^{-c} \\
f_2(a, b) &= q(4, 2) \cdot h_3 e^{-h_3 a} \cdot e^{-b} \\
&= \frac{1}{2} e^{-h_3 a} \cdot e^{-b} \\
f_3^+(a, b, c) &= q(4, 3) \cdot h_3 e^{-h_3 a} \cdot (q(3, 2) + q(3, 1)) \cdot h_2 e^{-h_2 c} \cdot e^{-(b-c)} \\
f_3(a, b) &= q(4, 3) \cdot h_3 e^{-h_3 a} \cdot (q(3, 2) + q(3, 1)) \cdot h_2 \cdot 2(1 - e^{-b/2}) \cdot e^{-b} \\
&= 2e^{-h_3 a} (1 - e^{-b/2}) \cdot e^{-b} \\
f_4^+(a, b, c) &= q(4, 3) \cdot h_3 e^{-h_3 a} \cdot (q(3, 2) + q(3, 1)) \cdot h_2 e^{-h_2 b} \cdot e^{-c} \\
f_4(a, b) &= q(4, 3) \cdot h_3 e^{-h_3 a} \cdot (q(3, 2) + q(3, 1)) \cdot h_2 e^{-h_2 b} \\
&= e^{-h_3 a} \cdot e^{-h_2 b}.
\end{aligned}$$

From this we can verify (66).

This argument is not so illuminating, but we can immediately derive the conditional distribution of CTCS(4) given that CTCS(3) is (\mathbf{t}, a, b) . Writing $g_i(c|a, b)$ for the conditional density of shape \mathbf{t}_i or $\hat{\mathbf{t}}_i$ and additional edge length c , and $p(\mathbf{t}_i|a, b) = \int g_i(c|a, b) dc$ for the conditional probability of shape \mathbf{t}_i or $\hat{\mathbf{t}}_i$, we have

$$\begin{aligned} g_1(c|a, b) &= \frac{\frac{1}{4}f_1^+(a, b, c)}{f(a, b)} = \frac{1}{3}e^{-c/3}; & p(\mathbf{t}_1|a, b) &= 1 - e^{-a/3} \\ g_2(c|a, b) &= \frac{\frac{1}{2}f_2^+(a, b, c)}{f(a, b)} = \frac{1}{3}e^{-a/3} \cdot e^{-c}; & p(\mathbf{t}_2|a, b) &= \frac{1}{3}e^{-a/3} \\ g_3(c|a, b) &= \frac{\frac{1}{4}f_3^+(a, b, c)}{f(a, b)} = \frac{1}{3}e^{-a/3} \cdot e^{-c/2}; & p(\mathbf{t}_3|a, b) &= \frac{2}{3}e^{-a/3}(1 - e^{-b/2}) \\ g_4(c|a, b) &= \frac{\frac{1}{2}f_4^+(a, b, c)}{f(a, b)} = \frac{2}{3}e^{-a/3}e^{-b/2} \cdot e^{-c}; & p(\mathbf{t}_4|a, b) &= \frac{2}{3}e^{-a/3} \cdot e^{-b/2}. \end{aligned}$$

One can now see that these are the conditional probabilities that arise from the growth algorithm in section 5.1, which we for convenience repeat:

Given a realization of CTCS(n) for some $n \geq 1$ (above, $n = 3$):

- Pick a uniform random bud; move up the path from the root toward that bud. A “stop” event occurs at rate = $1/(\text{size of sub-clade from current position})$.
- If “stop” before reaching the target bud, make a side-bud at that point, random on left or right. (As in \mathbf{t}_1 or \mathbf{t}_3 above.)
- Otherwise, extend the target bud into a branch of Exponential(1) length to make a bud-pair. (As in \mathbf{t}_2 or \mathbf{t}_4 above.)

Figure 12 indicated three of these possibilities ($\mathbf{t}_1, \mathbf{t}_3, \mathbf{t}_4$) when the chosen target bud was at the top right. The “rate” is $1/3$ until the side-bud, and then $1/2$. Note that case \mathbf{t}_2 arises as an “extend the target bud” for a different target bud.

6.8.2 The general step

To set up a calculation, we consider the side-bud addition case first, illustrated by the example in Figure 13, where the left diagram shows the relevant part of \mathbf{t}_n and the right diagram shows the side-bud addition making \mathbf{t}_{n+1} . The ℓ_i are edge-lengths and the (n_i) are clade sizes. The side-bud is attached to some edge, in Figure 13 an edge at edge-height 4 with length ℓ_4 and defining a clade of size $n_4 \geq 2$. The new bud splits that edge into edges of length α and $\ell_4 - \alpha$. The probability density function on a given tree is a product of terms for each edge. Table 1 shows the

terms for the edges where the terms differ between the two trees – these are only the edges on the path from the root to the added bud. The first three lines in Table 1 refer to the edges below the old edge into which the new bud is inserted, and the bottom line refers to that old edge.

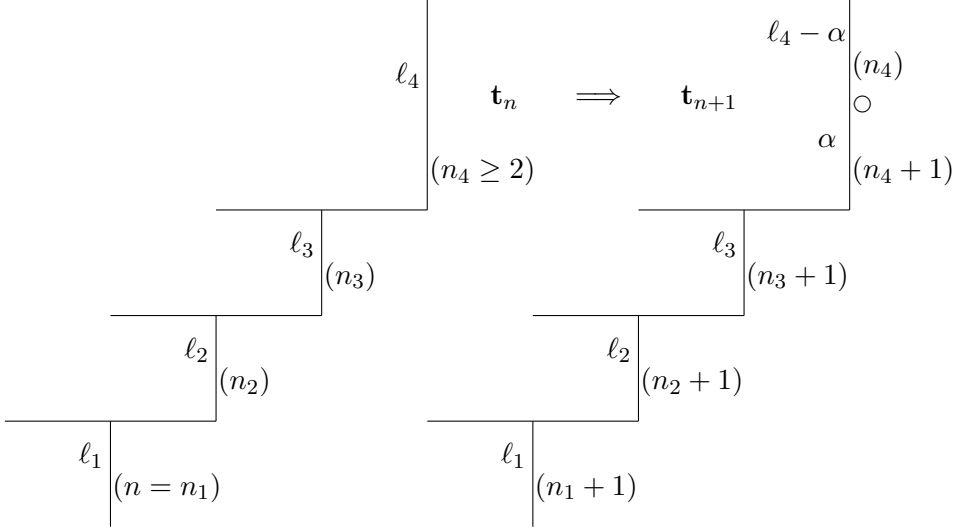


Figure 13: Growing via a side-bud addition

left tree	right tree
$h_{n_1-1} \exp(-h_{n_1-1} \ell_1) d\ell_1 \cdot q(n_1, n_2)$	$h_{n_1} \exp(-h_{n_1} \ell_1) d\ell_1 \cdot q(n_1 + 1, n_2 + 1)$
$h_{n_2-1} \exp(-h_{n_2-1} \ell_2) d\ell_2 \cdot q(n_2, n_3)$	$h_{n_2} \exp(-h_{n_2} \ell_2) d\ell_2 \cdot q(n_2 + 1, n_3 + 1)$
$h_{n_3-1} \exp(-h_{n_3-1} \ell_3) d\ell_3 \cdot q(n_3, n_4)$	$h_{n_3} \exp(-h_{n_3} \ell_3) d\ell_3 \cdot q(n_3 + 1, n_4 + 1)$
$h_{n_4-1} \exp(-h_{n_4-1} \ell_4) d\ell_4$	$h_{n_4} \exp(-h_{n_4} \alpha) d\alpha \cdot q(n_4 + 1, 1)$ $\cdot h_{n_4-1} \exp(-h_{n_4-1} (\ell_4 - \alpha)) d\ell_4$

Table 1: Differing terms in density product (side-bud case)

$h_{n_4-1} \exp(-h_{n_4-1} \ell_4) d\ell_4$	$h_{n_4} \exp(-h_{n_4} \ell_4) d\ell_4 \cdot q(n_4 + 1, 1)$ $\cdot h_1 \exp(-h_1 \beta) d\beta$
---	--

Table 2: Differing terms in density product (branch extension case)

Because $h_{n-1} q(n, k) = \frac{n}{2k(n-k)}$ the ratios right/left of each of the first 3 lines in

Table 1 equal

$$\frac{n_i + 1}{n_i} \cdot \frac{n_{i+1}}{n_{i+1} + 1} \cdot \exp(-\ell_i/n_i), \quad i = 1, 2, 3.$$

The corresponding ratio for the final term equals

$$\frac{n_4 + 1}{2n_4} \cdot \exp(-\alpha/n_4) d\alpha.$$

Combining terms, the ratio of densities equals

$$\frac{n + 1}{2n} \cdot \exp(-\ell_1/n_1 - \ell_2/n_2 - \ell_3/n_3 - \alpha/n_4) d\alpha.$$

In obtaining \mathbf{t}_n from \mathbf{t}_{n+1} we chose one of $n + 1$ buds to delete, so finally the conditional density of CTCS($n+1$) given CTCS(n) at $(\mathbf{t}_{n+1}|\mathbf{t}_n)$ equals

$$\frac{1}{2n} \cdot \exp(-\ell_1/n_1 - \ell_2/n_2 - \ell_3/n_3 - \alpha/n_4) d\alpha. \quad (67)$$

We need to check that this agrees with the inductive algorithm. According to the algorithm, the conditional density is a product of terms

- n_4/n : the chance that the target bud is in the relevant clade;
- $\exp(-\ell_1/n_1 - \ell_2/n_2 - \ell_3/n_3)$: the chance of not stopping before reaching the edge of length ℓ_4 ;
- $\frac{1}{n_4} \exp(-\alpha/n_4)d\alpha$: the chance of stopping in $d\alpha$;
- $1/2$: chance of placing side-bud on right side.

And this agrees with (67).

That was the side-bud addition case. Now consider the branch extension case, illustrated in Figure 14. In this case, \mathbf{t}_n has an edge terminating in two buds. Then \mathbf{t}_{n+1} is obtained by extending the branch by an extra edge of some length β to two terminal buds, leaving one bud as a side-bud. Comparing the densities of \mathbf{t}_n and \mathbf{t}_{n+1} in this case, the first 3 lines are the same as in Table 1, and the 4th is shown in Table 2. Following the previous argument we derive the conditional density in a format similar to (67):

$$\frac{1}{2n} \cdot \exp(-\ell_1/n_1 - \ell_2/n_2 - \ell_3/n_3 - \ell_4/n_4 - \beta) d\beta. \quad (68)$$

Again this agrees with the inductive algorithm. The third case, the side-bud extension, is similar.

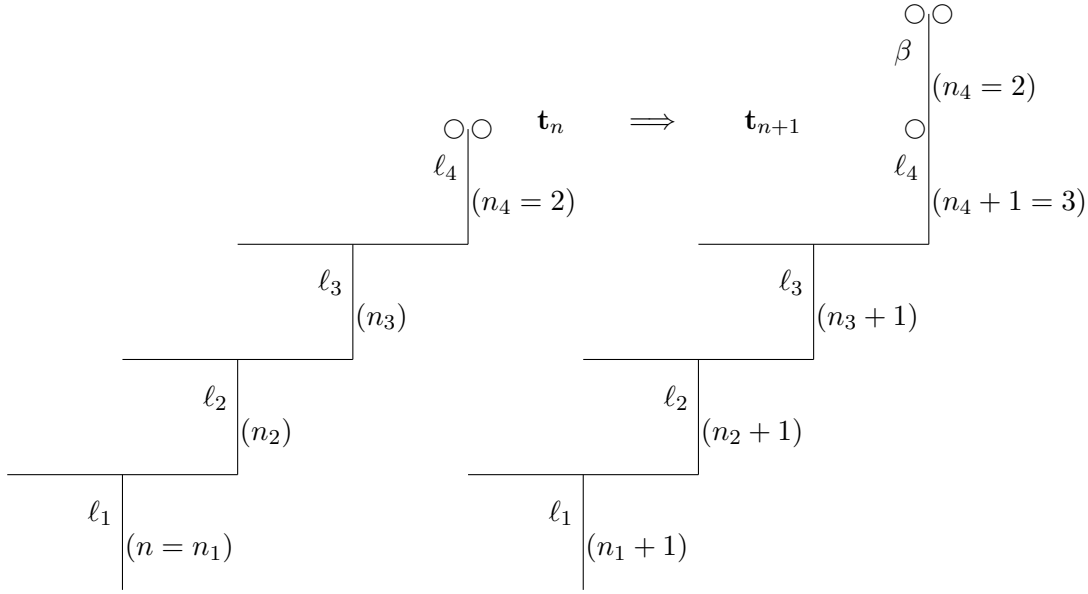


Figure 14: Growing via a branch extension

6.9 Alternative proof of the consistency property

The rate at which a clade of size m splits into two clades of sizes i and $m - i$ (taking the left subclade first, for definiteness) is

$$\hat{q}(m, i) := h_{m-1}q(m, i) = \frac{m}{2i(m-i)} = \frac{1}{2i} + \frac{1}{2(m-i)}, \quad 1 \leq i \leq m-1. \quad (69)$$

Consider $\text{CTCS}(n+1)$, but kill leaf $n+1$ and replace it with an invisible ghost. Consider a clade in the tree with m visible elements plus the ghost. This clade really has $m+1$ elements and thus splits with rate h_m in $\text{CTCS}(n+1)$, but the cases when only the ghost is split off from the rest is invisible. A visible split into subsets with j and $m-j$ visible elements may have the ghost in any of the two, and the rate is thus (taking into account the probability that the ghost appears in the proper subclade)

$$\begin{aligned} \frac{j+1}{m+1}\hat{q}(m+1, j+1) + \frac{m+1-j}{m+1}\hat{q}(m+1, j) &= \frac{j+1}{2(j+1)(m-j)} + \frac{m+1-j}{2j(m+1-j)} \\ &= \frac{1}{2(m-j)} + \frac{1}{2j} = \hat{q}(m, i). \end{aligned} \quad (70)$$

In other words, the ghost does not affect the visible splitting rates. Hence, if we delete leaf $n+1$ from $\text{CTCS}(n+1)$, we obtain $\text{CTCS}(n)$, which proves Theorem 7.

This construction leads to an alternative proof of the growth algorithm, as shown next.

6.9.1 The growth algorithm

We continue to consider $\text{CTCS}(n+1)$ with leaf $n+1$ replaced by an invisible ghost. In the argument above, we see from (70) that if a clade containing the ghost and m visible leaves splits into new clades of visible sizes j and $m-j$, then the ghost will be in the clade of size j with probability

$$\frac{1/2(m-j)}{\hat{q}(m,j)} = \frac{j}{m}. \quad (71)$$

In other words, the ghost moves as if it accompanies a uniformly chosen visible leaf in the clade. Note also that when the ghost belongs to a clade with m visible elements, it splits off on its own at the rate

$$\frac{2}{m+1}\hat{q}(m+1,1) = \frac{1}{m}. \quad (72)$$

(This follows also because the splitting rate in $\text{CTCS}(n+1)$ is h_m , of which the visible splits have rate h_{m-1} ; hence the rate is $h_m - h_{m-1}$.) This means that given $\text{CTCS}(n)$, the life of the ghost can (up to identity in distribution) be described by: Choose a leaf in $\text{CTCS}(n)$ uniformly at random, and follow the branch towards it. With rate $1/(\text{current size of the clade (excluding the ghost)})$, branch off alone; if the ghost reaches the chosen leaf, continue together with it and branch off from it with the same rate (now 1).

We may thus construct $\text{CTCS}(n+1)$ from $\text{CTCS}(n)$ by the procedure just described, but giving life to the ghost as leaf $n+1$. This gives precisely the growth algorithm in section 5. ■

6.10 A hidden symmetry?

From Proposition 6 and (16) we see that $\ell := \lim_n n^{-1}\mathbb{E}[L_n]$ and $a(2)$ are both equal to $6/\pi^2$. There are two different implications of “ $a(2) = \ell$ ”. First, it implies that (asymptotically) exactly half of the total length is in the “terminal” edges to a bud-pair. Second, in the inductive construction we expect that as $n \rightarrow \infty$ there are limit probabilities for the three types of placement of the new bud:

- p^\uparrow is the probability of a branch extension
- p^\rightarrow is the probability of a side-bud addition
- p^\nearrow is the probability of a side-bud extension.

Now observe

$$p^\uparrow + p^\nearrow = \ell$$

because these are the cases where the tree length increases by a mean length 1. And

$$2p^{\nearrow} = a(2)$$

because this is the only case where the number of buds in pairs increases, by 2.

So the assertion $\ell = a(2)$ is equivalent to the assertion $p^{\uparrow} = p^{\nearrow}$.

Open Problem 8 *Is the fact $p^{\uparrow} = p^{\nearrow}$ a consequence of some kind of symmetry for the shape of the tree?*

6.11 Proof of Lemma 9

It is easily seen from the inductive algorithm that a.s., as n grows to ∞ :

1. Infinitely many buds of height $< t$ are added, and thus $\Pi(t)_\ell \neq \emptyset$ for every $\ell \geq 1$, and
2. Once a clade $\Pi^{[n]}(t)_\ell$ is non-empty, new leaves will be added to it an infinite number of times.

The result follows. ■

6.12 Proof of Theorem 11

Consider the effect on the forest $F_t^{(n)}$ of adding a new leaf by the inductive algorithm. We have the following cases:

- (i) If the algorithm stops at height $u < t$, then CTCS(n) gets a new leaf (bud) there, which means that $F_t^{(n)}$ gets a new tree consisting of a root only.
- (ii) If the target leaf has height $\geq t$ and the algorithm does not stop before reaching height t , then the algorithm will continue in the tree containing the target exactly as it would if acting on this tree separately. All other trees in $F_t^{(n)}$ remain unchanged. Note also that the probability of reaching height t is the same for all target leaves in a given tree in $F_t^{(n)}$; hence the conditional distribution of the target leaf, given the tree in $F_t^{(n)}$ that it belongs to, is uniform.
- (iii) If the target leaf has height $< t$ and the algorithm does not stop until reaching the target, then the target leaf is extended into a branch of Exponential(1) length L ending with a bud-pair.

If $u + L < t$, then the two buds in the pair define separate singleton trees in $F_t^{(n+1)}$, and thus the net effect is to add a new tree consisting of a root only to $F_t^{(n)}$.

On the other hand, if $u + L \geq t$, then the tree in $F_t^{(n)}$ consisting of the target leaf (only) becomes a tree with two leaves at the end of a branch of length $L + u - t$. Since the exponential distribution has no memory, also this branch length has Exponential(1) (conditional) distribution, and thus this tree has the distribution of CTCS(2).

All cases conform to the description in the statement. ■

6.13 Proof of Theorem 12

We prove the theorem in 3 steps.

Step 1. Y_t is a subordinator. Recall that $K_{t,1}^{(n)}$ is the size of the first clade of CTCS(n) at time t . Consider two fixed times t and $t + h$, where $h > 0$. Then Theorem 11 and (22) imply that a.s., as $n \rightarrow \infty$,

$$\frac{K_{t+h,1}^{(n)}}{K_{t,1}^{(n)}} \rightarrow P'_{h,1}, \quad (73)$$

where $P'_{h,1}$ is a copy of $P_{h,1}$ that is independent of $P_{t,1}$. Consequently, a.s.

$$\frac{K_{t+h,1}^{(n)}}{n} = \frac{K_{t+h,1}^{(n)}}{K_{t,1}^{(n)}} \cdot \frac{K_{t,1}^{(n)}}{n} \rightarrow P'_{h,1} P_{t,1} \quad (74)$$

and thus

$$P_{t+h,1} = P_{t,1} P'_{h,1}. \quad (75)$$

Hence, $Y_t := -\log P_{t,1}$ is an increasing stochastic process with stationary independent increments, i.e., a subordinator. Note that $Y_t < \infty$ a.s. since $P_{t,1} > 0$ by Theorem 10.

Step 2. The Lévy measure is given by (23). In order to verify this, we calculate moments. Let $k \geq 0$. By the paintbox construction in Theorem 10,

$$\mathbb{P}(\Pi(t)_1 \cap [k+1] = [k+1] \mid (P_{t,\ell})_{\ell=1}^{\infty}) = \sum_{\ell=1}^{\infty} P_{t,\ell}^{k+1}. \quad (76)$$

Furthermore, also as a consequence of the paintbox construction, $P_{t,1}$ has the same distribution as a size-biased sample of $(P_{t,\ell})_{\ell=1}^{\infty}$ [11, Proposition 2.8], and thus [11, Corollary 2.4]

$$\mathbb{E}[P_{t,1}^k] = \mathbb{E}\left[\sum_{\ell=1}^{\infty} P_{t,\ell}^{k+1}\right]. \quad (77)$$

Consequently, (77) and (76) together with the definition of $\Pi(t)_1$ in section 5.3 yield

$$\begin{aligned}\mathbb{E}[P_{t,1}^k] &= \mathbb{P}(\Pi(t)_1 \cap [k+1] = [k+1]) \\ &= \mathbb{P}(2, 3, \dots, k+1 \in \Pi(t)_1) \\ &= \mathbb{P}(\text{CTCS}(k+1) \text{ has no branchpoint with height } \leq t).\end{aligned}\quad (78)$$

The latter event occurs if and only if for each $j \leq k$, in the inductive construction by the growth algorithm of $\text{CTCS}(j+1)$ from $\text{CTCS}(j)$, there is no stop at height $\leq t$. Since the subclade at the current position then has size j for all times $\leq t$, the probability of this happening at step j , given that it has happened so far, is $\exp(-t/j)$. Consequently,

$$\mathbb{E}[P_{t,1}^k] = \prod_{j=1}^k e^{-t/j} = \exp\left(-t \sum_{j=1}^k \frac{1}{j}\right) = e^{-h_k t}.\quad (79)$$

On the other hand, let \mathcal{Y}_t be the subordinator with Lévy measure given by (23). Then, by definition, for any real $s \geq 0$,

$$\mathbb{E}[e^{-s\mathcal{Y}_t}] = \exp\left(-t \int_0^\infty (1 - e^{-sx}) f_\infty(x) dx\right) = \exp\left(-t \int_0^\infty \frac{1 - e^{-sx}}{1 - e^{-x}} e^{-x} dx\right).\quad (80)$$

In particular, if $s = k$ is an integer,

$$\begin{aligned}\mathbb{E}[(e^{-\mathcal{Y}_t})^k] &= \mathbb{E}[e^{-k\mathcal{Y}_t}] = \exp\left(-t \int_0^\infty \frac{e^{-x} - e^{-(k+1)x}}{1 - e^{-x}} dx\right) = \exp\left(-t \int_0^\infty \sum_{j=1}^k e^{-jx} dx\right) \\ &= \exp\left(-t \sum_{j=1}^k \frac{1}{j}\right) = e^{-h_k t}.\end{aligned}\quad (81)$$

Consequently, for any $t \geq 0$, (79) and (81) show $\mathbb{E}[P_{t,1}^k] = \mathbb{E}[(e^{-\mathcal{Y}_t})^k]$ for all $k \geq 1$, and thus, by the method of moments (since the random variables on both sides are bounded, with values in $[0, 1]$) $P_{t,1} \stackrel{d}{=} e^{-\mathcal{Y}_t}$. Thus $Y_t = -\log P_{t,1} \stackrel{d}{=} \mathcal{Y}_t$.

This calculation is for a fixed $t \geq 0$, but we know that the process (Y_t) is a subordinator, and thus the distribution of the entire process is determined by, say, the distribution of Y_1 .

Step 3. The moment formula. For any complex s with $\Re s > -1$, we have [50, 5.9.16] (as is easily verified by standard arguments)

$$\int_0^\infty \frac{1 - e^{-sx}}{1 - e^{-x}} e^{-x} dx = \int_0^\infty \frac{e^{-x} - e^{-(s+1)x}}{1 - e^{-x}} dx = \psi(s+1) - \psi(1),\quad (82)$$

generalizing the formula for integer s in (81). Hence, (80) yields, for $t \geq 0$ and $\Re s > -1$,

$$\mathbb{E}[P_{t,1}^s] = \mathbb{E}[e^{-sY_t}] = \mathbb{E}[e^{-s\mathcal{Y}_t}] = e^{-t(\psi(s+1)-\psi(1))}, \quad (83)$$

which shows (24) and completes the proof of the theorem. \blacksquare

6.14 The Mellin transform argument

Here we show how to derive Theorem 5 from the exchangeable representation and Theorem 12.

For $j \geq 2$, let $N_j^{(n)}$ be the number of internal nodes of CTCS(n) that have exactly j leaves as descendants. Similarly, let $N_j^{(n)}(t)$ be the number of clades of CTCS(n) at time t that have size exactly j . Let

$$e_j^{(n)} := \mathbb{E}[N_j^{(n)}], \quad e_j^{(n)}(t) := \mathbb{E}[N_j^{(n)}(t)].$$

The integral $\int_0^\infty N_j^{(n)}(t) dt$ equals the sum of the lifetimes of all clades of size j that ever appear in CTCS(n); because these lifetimes have expectation $1/h_{j-1}$ (and are independent of the structure), we have

$$\int_0^\infty e_j^{(n)}(t) dt = \mathbb{E} \int_0^\infty N_j^{(n)}(t) dt = \frac{1}{h_{j-1}} \mathbb{E} N_j^{(n)} = \frac{e_j^{(n)}}{h_{j-1}}. \quad (84)$$

As noted previously,

$$a(n, j) = \frac{j}{n} e_j^{(n)} \quad (85)$$

so to prove Theorem 5 it will suffice to study the behavior of $e_j^{(n)}$.

To start to calculate $e_j^{(n)}$, use the paintbox construction in Theorem 10 to see that

conditioned on $(P_{t,\ell})_{\ell=1}^\infty$, the probability that a given set of j leaves form a clade at time t equals $\sum_{\ell} P_{t,\ell}^j (1 - P_{t,\ell})^{n-j}$.

Thus, by recalling that $P_{t,1}$ can be regarded as a size-biased sample of $(P_{t,\ell})_{\ell=1}^\infty$ [11, Corollary 2.4], we see

$$e_j^{(n)}(t) = \binom{n}{j} \mathbb{E} \left[\sum_{\ell} P_{t,\ell}^j (1 - P_{t,\ell})^{n-j} \right] = \binom{n}{j} \mathbb{E} [P_{t,1}^{j-1} (1 - P_{t,1})^{n-j}]. \quad (86)$$

Let μ be the infinite measure on $[0, 1]$ given by

$$\mu := \int_0^\infty \mathcal{L}(P_{t,1}) dt. \quad (87)$$

Then (86) yields

$$\int_0^\infty e_j^{(n)}(t) dt = \binom{n}{j} \int_0^1 x^{j-1} (1-x)^{n-j} d\mu(x) \quad (88)$$

and thus

$$\frac{1}{n} \int_0^\infty e_j^{(n)}(t) dt \sim \frac{n^{j-1}}{j!} \int_0^1 x^{j-1} (1-x)^{n-j} d\mu(x) \quad \text{as } n \rightarrow \infty.$$

Theorem 12 tells us the moments of the measure μ : by integrating (83)

$$\int_0^1 x^{s-1} d\mu(x) = \frac{1}{\psi(s) - \psi(1)}, \quad \Re s > 1. \quad (89)$$

Granted Lemma 13 (proved below), we complete a proof of Theorem 5 as follows. By (84), (88) and Lemma 13, we have

$$\frac{1}{h_{j-1}} \frac{e_j^{(n)}}{n} = \frac{1}{n} \int_0^\infty e_j^{(n)}(t) dt = \frac{1}{n} \binom{n}{j} \int_0^1 x^{j-1} (1-x)^{n-j} f(x) dx. \quad (90)$$

Substitute $f(x)$ from (27). The main term becomes, using a standard beta integral,

$$\begin{aligned} \frac{1}{n} \binom{n}{j} \int_0^1 x^{j-1} (1-x)^{n-j} \frac{6}{\pi^2} x^{-1} dx &= \frac{6}{\pi^2} \frac{1}{n} \binom{n}{j} \int_0^1 x^{j-2} (1-x)^{n-j} dx \\ &= \frac{6}{\pi^2} \frac{1}{n} \binom{n}{j} \frac{\Gamma(j-1)\Gamma(n-j+1)}{\Gamma(n)} \\ &= \frac{6}{\pi^2} \frac{1}{n} \binom{n}{j} \frac{(j-2)!(n-j)!}{(n-1)!} \\ &= \frac{6}{\pi^2} \frac{1}{j(j-1)}. \end{aligned} \quad (91)$$

The contribution from the error term in (27) has absolute value at most, letting C denote unimportant constants (not necessarily the same), and using $-\log x > 1-x$,

$$\begin{aligned} C \frac{1}{n} \binom{n}{j} \int_0^1 x^{j-1} (1-x)^{n-j} x^{-s_1} (1+|\log x|^{-1}) dx &\leq C n^{j-1} \int_0^1 x^{j-s_1-1} (1-x)^{n-j-1} dx \\ &\leq C n^{j-1} \int_0^\infty x^{j-s_1-1} e^{-(n-j-1)x} dx \\ &= C n^{j-1} (n-j-1)^{-j+s_1} \\ &= O(n^{s_1-1}). \end{aligned} \quad (92)$$

This is $o(1)$ as $n \rightarrow \infty$, and thus from (90) and (91), for every fixed $j \geq 2$,

$$\frac{e_j^{(n)}}{n} \rightarrow \frac{6}{\pi^2} \frac{h_{j-1}}{j(j-1)}. \quad (93)$$

Then by (85) we get the assertion of Theorem 5:

$$a(n, j) \rightarrow \frac{6}{\pi^2} \frac{h_{j-1}}{j-1} =: a(j). \quad (94)$$

■

6.15 Proof of Lemma 13 by Mellin inversion

We repeat the statement of Lemma 13.

Lemma 13. Let μ be the infinite measure on $[0, 1)$ having the Mellin transform (89). Then μ is absolutely continuous, with a continuous density $f(x)$ on $(0, 1)$ that satisfies

$$f(x) = \frac{6}{\pi^2 x} + O(x^{-s_1} + x^{-s_1} |\log x|^{-1}), \quad (95)$$

uniformly for $x \in (0, 1)$, where $s_1 \doteq -0.567$ is the largest negative root of $\psi(s) = \psi(1)$. In particular, for $x \in (0, \frac{1}{2})$ say,

$$f(x) = \frac{6}{\pi^2 x} + O(x^{-s_1}) \text{ as } x \downarrow 0. \quad (96)$$

Proof. We begin by noting that the Mellin transform $1/(\psi(s) - \psi(1))$ in (89) extends to a meromorphic function in the entire complex plane. The poles are the roots of

$$\psi(s) = \psi(1). \quad (97)$$

Obviously, $s_0 := 1$ is a pole. Its residue is

$$\text{Res}_{s=1} \frac{1}{\psi(s) - \psi(1)} = \frac{1}{\psi'(1)} = \frac{6}{\pi^2}, \quad (98)$$

using the well known formula $\psi'(1) = \pi^2/6$ [50, 5.4.12] (see also (113) below). As shown in Lemma 21 below the other poles are real and negative, and thus can be ordered $0 > s_1 > s_2 > \dots$. In particular, there are no other poles in the half-plane $\Re s > s_1$, with $s_1 \doteq -0.567$.

We cannot immediately use standard results on Mellin inversion²¹ (as in [23, Theorem 2(i)]) because the Mellin transform in (89) decreases too slowly as $\Im s \rightarrow \pm\infty$ to be integrable on a vertical line $\Re s = c$. In fact, Stirling's formula implies (see e.g. [50, 5.11.2]) that

$$\psi(s) = \log s + o(1) = \log |s| + O(1) = \log |\Im s| + O(1) \quad (99)$$

as $\Im s \rightarrow \infty$ with s in, for example, any half-plane $\Re s \geq c$.

We overcome this problem by differentiating the Mellin transform, but we first subtract the leading term corresponding to the pole at 1. Since μ is an infinite measure, we first replace it by ν defined by $d\nu(x) = x d\mu(x)$; note that ν is also a measure on $[0, 1)$, and (89) shows that ν is a finite measure.

Next, define ν_0 as the measure $(6/\pi^2) dx$ on $[0, 1)$, and let ν_Δ be the (finite) signed measure $\nu - \nu_0$. Then ν_Δ has the Mellin transform, by (89),

$$\begin{aligned} \widetilde{\nu}_\Delta(s) &:= \int_0^1 x^{s-1} d\nu_\Delta(x) = \int_0^1 x^s d\mu(x) - \frac{6}{\pi^2} \int_0^1 x^{s-1} dx \\ &= \frac{1}{\psi(s+1) - \psi(1)} - \frac{6}{\pi^2 s}, \quad \Re s > 0. \end{aligned} \quad (100)$$

We may here differentiate under the integral sign, which gives

$$\widetilde{\nu}_\Delta'(s) := \int_0^1 (\log x) x^{s-1} d\nu_\Delta(x) \quad (101)$$

$$= -\frac{\psi'(s+1)}{(\psi(s+1) - \psi(1))^2} + \frac{6}{\pi^2 s^2}, \quad \Re s > 0. \quad (102)$$

The Mellin transform $\widetilde{\nu}_\Delta(s)$ extends to a meromorphic function in \mathbb{C} with (simple) poles $(s_i - 1)_1^\infty$; note that there is no pole at $s_0 - 1 = 0$, since the residues there of the two terms in (100) cancel by (98). Furthermore, the formula (102) for $\widetilde{\nu}_\Delta'(s)$ holds for all s (although the integral in (101) diverges unless $\Re s > 0$).

For any real c we have, on the vertical line $\Re s = c$, as $\Im s \rightarrow \pm\infty$, that $\psi(s) \sim \log |s|$ by (99), and also, by careful differentiation of (99) or by [50, 5.15.8] that $\psi'(s) \sim s^{-1}$. It follows from (102) that $\widetilde{\nu}_\Delta'(s) = O(|s|^{-1} \log^{-2} |s|)$ on the line $\Re s = c$, for $|\Im s| \geq 2$ say, and thus $\widetilde{\nu}_\Delta'$ is integrable on this line unless c is one of the poles $s_i - 1$. In particular, taking $c = 1$ and thus $s = 1 + ui$ ($u \in \mathbb{R}$), we see that the function

$$\widetilde{\nu}_\Delta'(1 + iu) = \int_0^1 x^{iu} \log(x) d\nu_\Delta(x) \quad (103)$$

²¹And we cannot use [23, Theorem 2(ii)] since we do not know that μ has a density that is locally of bounded variation.

is integrable. The change of variables $x = e^{-y}$ shows that the function (103) is the Fourier transform of the signed measure on \mathbb{R}_+ that corresponds to $\log(x) d\nu_\Delta(x)$. This measure on \mathbb{R}_+ is thus a finite signed measure with integrable Fourier transform, which implies that it is absolutely continuous with a continuous density. Reversing the change of variables, we thus see that the signed measure $\log(x) d\nu_\Delta(x)$ is absolutely continuous with a continuous density on $(0, 1)$. Moreover, denoting this density by $h(x)$, we obtain the standard inversion formula for the Mellin transform [23, Theorem 2(i)], [50, 1.14.35]:

$$h(x) = \frac{1}{2\pi i} \int_{c-\infty i}^{c+\infty i} x^{-s} \widetilde{\nu}_\Delta'(s) ds, \quad x > 0, \quad (104)$$

with $c = 1$. Furthermore, the integrand in (104) is analytic in the half-plane $\Re s > s_1 - 1$, and the estimates above of $\psi(s)$ and $\psi'(s)$ are uniform for $\Re s$ in any compact interval and, say, $|\Im s| \geq 2$. Consequently, we may shift the line of integration in (104) to any $c > s_1 - 1$. Taking absolute values in (104), and recalling that $\widetilde{\nu}_\Delta'(s)$ is integrable on the line, then yields

$$h(x) = O(x^{-c}) \quad (105)$$

for any $c > s_1 - 1$.

Reversing the transformations above, we see that ν_Δ has the density $(\log x)^{-1}h(x)$, and thus ν has the density $(\log x)^{-1}h(x) + 6/\pi^2$, and, finally, that μ has the density

$$f(x) := \frac{d\mu}{dx} = \frac{1}{x} \frac{d\nu}{dx} = \frac{6}{\pi^2 x} + \frac{1}{x \log x} h(x), \quad 0 < x < 1. \quad (106)$$

Furthermore, (106) and (105) have the form of the claimed estimate (95), although with the weaker error term $O(x^{-s_1-\varepsilon} |\log x|^{-1})$ for any $\varepsilon > 0$.

To obtain the (stronger) claimed error term, we note that the residue of $\nu_\Delta(s)$ at $s_1 - 1$ is $r_1 := 1/\psi'(s_1)$. Let ν_1 be the measure $r_1 x^{1-s_1} dx$ on $[0, 1)$; then ν_1 has Mellin transform

$$\widetilde{\nu}_1(s) = r_1 \int_0^1 x^{s-1} x^{1-s_1} dx = \frac{r_1}{s+1-s_1}, \quad \Re s > s_1 - 1. \quad (107)$$

It follows from (100) and (107) that the signed measure $\nu - \nu_0 - \nu_1 = \nu_\Delta - \nu_1$ has the Mellin transform

$$\frac{1}{\psi(s+1) - \psi(1)} - \frac{6}{\pi^2 s} - \frac{r_1}{s+1-s_1}, \quad (108)$$

which is an analytic function in the half plane $\Re s > s_2 - 1$. Hence, the same argument as above yields the estimate

$$f(x) = \frac{6}{\pi^2 x} + \frac{1}{\psi'(s_1)} x^{-s_1} + O(x^{-s_2 - \varepsilon} |\log x|^{-1}), \quad x \downarrow 0, \quad (109)$$

for any $\varepsilon > 0$, which in particular yields (95). ■

Remark 19 We may continue the argument above further and subtract similar terms for any number of poles; this leads to the estimate, for any $N \geq 1$,

$$f(x) = \frac{6}{\pi^2 x} + \sum_{i=1}^N \frac{1}{\psi'(s_i)} x^{-s_i} + O(x^{-s_N} |\log x|^{-1}), \quad 0 < x < 1, \quad (110)$$

with, as above, $0 > s_1 > s_2 > \dots$ denoting the negative roots of $\psi(s) = \psi(1)$.

Remark 20 Although the function $h(x)$ is continuous also at $x = 1$ (and thus $h(1) = 0$), the density $f(x)$ diverges as $x \nearrow 1$ because of the factor $\log x$ in the denominator in (106); in fact, it can be shown by similar arguments that

$$f(1 - y) \sim \frac{1}{y |\log y|^2}, \quad y \searrow 0. \quad (111)$$

Hence, the error term in (95) cannot be simplified as in (96) on the entire interval $(0, 1)$.

6.15.1 A lemma on the digamma function

Lemma 21 *The roots of the equation $\psi(s) = \psi(1)$ are all real and can be enumerated in decreasing order as $s_0 = 1 > s_1 > s_2 > \dots$, with $s_i \in (-i, -(i - 1))$ for $i \geq 1$. Numerically, $s_1 \doteq -0.5673537531$ and $s_2 \doteq -1.628460873$.*

Proof. Recall that $\psi(s)$ is a meromorphic function of s , with poles at $0, -1, -2, \dots$. For any other complex s we have the standard formulas [50, 5.7.6 and 5.15.1]

$$\psi(s) = -\gamma + \sum_{k=0}^{\infty} \left(\frac{1}{k+1} - \frac{1}{k+s} \right), \quad (112)$$

$$\psi'(s) = \sum_{k=0}^{\infty} \frac{1}{(k+s)^2}. \quad (113)$$

If $\Im s > 0$, then $\Im(1/(k+s)) < 0$ for all k and thus (112) implies $\Im \psi(s) > 0$. Similarly, if $\Im s < 0$, then $\Im \psi(s) < 0$. Consequently, all roots of $\psi(t) = \psi(1)$ are real.

For real s , (113) shows that $\psi'(s) > 0$. We can write $\mathbb{R} \setminus \{\text{the poles}\} = \bigcup_{i=0}^{\infty} I_i$ with $I_0 := (0, \infty)$ and $I_i := (-i, -(i-1))$ for $i \geq 1$; it then follows that $\psi(s)$ is strictly increasing in each interval I_i . Moreover, by (112) (or general principles), at the poles we have the limits $\psi(-i-0) = +\infty$ and $\psi(-i+0) = -\infty$ ($i \geq 0$). Consequently, $\psi(s) = \psi(1)$ has exactly one root s_i in each I_i , and obviously the positive root is $s_0 = 1$. (See also the graph of $\psi(s)$ in [50, Figure 5.3.3].)

Remark 22 The lemma and its proof extend to the equation $\psi(s) = a$ for any real a (using the fact that $\psi(s) \rightarrow \infty$ as $s \nearrow +\infty$), except that the values of s_i are different. See [50, §5.4(iii)] for the case $a = 0$.

7 Further aspects and open problems

There is an extensive literature (see e.g. [14, 39, 43, 46]) on many different aspects of many different models of random trees. In addition to the specific Open Problems mentioned already, there are many further aspects of our model that could be studied. We outline a few in this section.

As mentioned in section 4.3, the model was motivated by our small-scale study of real-world phylogenetic trees in [9] suggesting that, amongst all splits of clades of size m , the median size of the smaller subclade scales roughly as $m^{1/2}$. The recent monograph [22] surveys various *tree balance indices* designed to quantify such imbalance:

Open Problem 9 *Study the distribution of other indices for DTCS(n).*

Because our data studies of splitting and of the fringe distributions (Figure 9) were small-scale:

Open Problem 10 *Repeat these data studies on a larger scale and for other indices.*

Though we do not expect the model to provide quantitatively accurate matches to real data, the point is that more elaborate biologically-motivated models of the kind described in [42, 55] typically have real-valued parameters fitted to the individual tree data; how much do they improve on our zero-parameter model? In this context our asymptotics are irrelevant – one can just simulate DTCS(n) numerically.

7.1 Inspiration from the drawn cladogram representation

A perhaps novel aspect of random trees arises from considering how cladograms are actually drawn on paper, as illustrated in Figure 6. In the familiar models of

random trees starting with the Galton-Watson tree, it is natural to study the *width profile process*, the number of vertices at each height from the root [15]. In contrast a cladogram is drawn with all the leaves at the same “level zero”. So one could measure “height” with reference to that level, but this depends on precisely how one draws the cladogram.

There is in fact a convention implicit in Figure 6. Each clade-split $\gamma \rightarrow (\gamma_1, \gamma_2)$, is represented by a horizontal line at some *draw-height* $\text{dh}(\gamma)$. The draw-height depends on the shape of the subtree at γ , not merely on its size $|\gamma|$. For the usual convention, setting $\text{dh}(\gamma) = 0$ for a leaf (where $|\gamma| = 1$), we define dh inductively²² for $|\gamma| > 1$:

$$\gamma \rightarrow (\gamma_1, \gamma_2) : \quad \text{dh}(\gamma) = 1 + \max(\text{dh}(\gamma_1), \text{dh}(\gamma_2)). \quad (114)$$

In particular, if $|\gamma| = 2$ then $\text{dh}(\gamma) = 1$, and if $|\gamma| = 3$ then $\text{dh}(\gamma) = 2$, but for larger clades, $\text{dh}(\gamma)$ is not determined by the size: a clade of size 4 may have draw-height = 2 or 3, and a clade of size 8 may have draw-height = 3 or 4 or 5 or 6 or 7.

Now consider the draw-height $\text{dh}(\mathbf{t})$ of a finite clade tree \mathbf{t} , that is the draw-height of the root split. It is easy to see that this equals the height of \mathbf{t} in its DTCS(n) representation, that is the largest number of edges in the path from the root to a leaf. (Indeed the recursion for tree height is exactly (114).) For a leaf at this maximal height, the draw-heights upwards from the leaf take successive integer values $0, 1, 2, \dots, \text{dh}(\mathbf{t})$. For a leaf at lesser height, the difference of its height from the maximal height equals the number of missing integers in the draw-heights along the path from that leaf.

One feature of interest is the *drawn length* $\text{dl}(\gamma)$ of the cladogram representation γ of a tree, that is the sum of lengths of the vertical lines in the cladogram. This satisfies a recursion: for a split $\gamma_m \rightarrow (\gamma_i, \gamma_{m-i})$,

$$\text{dl}(\gamma_m) = \text{dl}(\gamma_i) + \text{dl}(\gamma_{m-i}) + 2 + |\text{dh}(\gamma_{m-i}) - \text{dh}(\gamma_i)|. \quad (115)$$

What is the drawn length $\text{dl}(\text{DTCS}(n))$ in our model?

Here is a heuristic analysis of $\overline{\text{DL}}_n := \mathbb{E}[\text{dl}(\text{DTCS}(n))]$. Write

$$\overline{\text{DH}}_n := \mathbb{E}[\text{dh}(\text{DTCS}(n))] \sim c \log^2 n \quad (116)$$

as in Open Problem 7. In our model the increment (115) is dominated by the contribution from uneven splits, so for $i < m/2$ we approximate the last term in (115) as $|\text{dh}(\gamma_{m-i}) - \text{dh}(\gamma_i)| \approx \text{dh}(\gamma_{m-i}) - \text{dh}(\gamma_i)$. Taking expectations and using

²²The “maximum” in this rule is somewhat reminiscent of the classical *Horton–Strahler* statistic [12] in river networks, though we do not see any precise relation. See [2] for a recent connection with the Brownian CRT in the context of asymptotics of uniform binary trees.

(115) recursively leads roughly to

$$\begin{aligned}
n^{-1}\overline{DL}_n &\approx 2 \sum_{m=2}^n a(n, m) \sum_{i=1}^{m/2} q(m, i)(2 + \overline{DH}_{m-i} - \overline{DH}_i) \\
&\approx 4c \sum_{m=2}^n m^{-1} \log m \sum_{i=1}^{m/2} q(m, i)(2 + c(\log^2(m-i) - \log^2 i)) \\
&\approx 2c \sum_{m=2}^n \sum_{i=1}^{m/2} \frac{1}{i(m-i)} (2 + c(\log^2(m-i) - \log^2 i)) \\
&\approx c^* \sum_{m=2}^n m^{-1} \log^3 m.
\end{aligned} \tag{117}$$

This leads to

Open Problem 11 *Prove that \overline{DL}_n grows roughly like $n \log^4 n$.*

In more detail, one could consider the analog of the width process mentioned earlier, illustrated in Figure 15.

Open Problem 12 *What can we say about the cladogram width profile process $(W(h), h \geq 0)$ for DTCS(n), for the number $W(h)$ of vertical lines that cross an interval $(h, h+1)$, that is the number of clades with draw-height $\leq h$ that arise as a split of a clade with draw-height $\geq h+1$?*

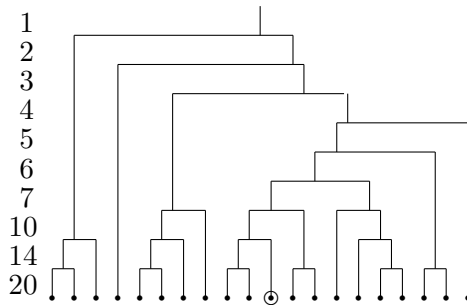


Figure 15: Width profile for the cladogram in Figure 5.

7.2 Powers of subtree sizes

Another aspect of random trees that has been studied in other models (for instance in [20, 21] for the model of conditioned Galton–Watson trees conditioned on total size n) is the sum of p -powers of subtree sizes. Our work provides some results and conjectures for that quantity $SS_n^{(p)}$ in our model, that is

$$SS_n^{(p)} := \sum_{j=2}^n N_n(j) j^p$$

where $N_n(j)$ is the number of size- j clades that ever arise in our model. By (15) and Theorem 5 we have

$$\mathbb{E}[N_n(j)] = na(n, j)/j \sim na(j)/j.$$

So for $-\infty < p < 1$ we expect that

$$n^{-1} \mathbb{E}[SS_n^{(p)}] = \sum_{j \geq 2} a(n, j) j^{p-1} \rightarrow \sum_{j \geq 2} a(j) j^{p-1} < \infty. \quad (118)$$

For $p = 1$ we have the identity, conditioning on the random tree \mathbb{T}_n ,

$$SS_n^{(1)} = n \cdot \mathbb{E}[L_n | \mathbb{T}_n]$$

and so by (11)

$$\mathbb{E}[SS_n^{(1)}] \sim \frac{n}{2\zeta(2)} \log^2 n. \quad (119)$$

For $p = 2$ we are dealing with the discrete time analog $(Q_n^{hop}(t), t = 0, 1, 2, \dots)$ of the sum of squares of clade sizes in section 6.1. Instead of the exact formulas there, we have an approximation

$$\mathbb{E}[Q_n(t) - Q_n(t+1) | \mathcal{F}_t] \approx Q_n(t) / \log n, \quad t = O(\log n)$$

leading to

$$\mathbb{E}[Q_n(t)] \approx n^2 \exp(-t / \log n), \quad t = O(\log n).$$

So heuristically

$$\mathbb{E}[SS_n^{(2)}] \approx \sum_t (\mathbb{E}[Q_n(t)] - n) \approx n^2 \log n. \quad (120)$$

In fact [20, 21] study also complex powers α , and as work-in-progress we are studying

Open Problem 13 *Give a detailed analysis of $SS_n^{(\alpha)}$ in our model.*

7.3 Analogies with and differences from the Brownian CRT

The best known continuous limit of finite random tree models is the Brownian continuum random tree (CRT) [4, 5, 18, 25], which is a scaling limit of conditioned Galton-Watson trees and other “uniform random tree” models. How does that compare with our $\text{CTCS}(\infty)$ model?

(a) The most convenient formalization of the Brownian CRT is as a random *measured metric space*, with the Gromov-Hausdorff-Prokhorov topology [1] on the set of all such spaces. So one automatically has a notion of convergence in distribution. Our formalization of $\text{CTCS}(\infty)$ via exchangeable partitions is less amenable to rephrasing as a random element of some metric space.

(b) Our consistency result, that $\text{CTCS}(n)$ is consistent as n increases, and exchangeable over the random leaves, constitutes one general approach to the construction of continuum random trees (CRTs) [5, 18].

(c) Our explicit inductive construction is analogous to the line-breaking construction of the Brownian CRT [4] and stable trees [26].

(d) Haas et al [31] and subsequent work such as [30] have given a detailed general treatment of self-similar fragmentations via exchangeable partitions, though the focus there is on characterizations and on models like the $-2 < \beta < -1$ case of the beta-splitting model (18). On the range $-2 < \beta < -1$, such models have limits which are qualitatively analogous to the Brownian continuum random tree, which is the case $\beta = -2$. But how this general abstract theory applies to explicit quantitative aspects of our specific $\beta = -1$ tree model seems a little hard to extract.

(e) We do not know if there is any relation between $\text{CTCS}(\infty)$ and the *stable trees* whose construction is studied in [16, 26].

(f) The Brownian CRT has a certain “local and global limits are consistent” property, as follows. That CRT is the scaling limit of certain discrete random tree models, and is encoded by Brownian excursion, and the local weak limit of those discrete models is a discrete infinite tree encoded by random walk-like processes. However these two limit processes are consistent in the following sense: the local behavior of the CRT around a typical point is another continuum tree encoded by the two-sided Bessel(3) process on \mathbb{R} , and this process is also the scaling limit of the discrete infinite tree arising as the local weak limit. In our CTCS model, the relationship between $\text{CTCS}(\infty)$ as a scaling limit, and the fringe distribution as a local limit, is rather harder to describe (cf. the section 5.6 comment that one can derive the latter from the former). It is intuitively clear that there is a scaling limit of the discrete fringe process itself, the limit being representable as a point process of branchpoint positions.

Open Problem 14 *Study that rescaled process.*

(g) It is implausible that $\text{CTCS}(\infty)$ is as “universal” a limit as the Brownian CRT has proved to be, but nevertheless one can ask

Open Problem 15 *Are there superficially different discrete models whose limit is the same $\text{CTCS}(\infty)$?*

The key feature of our model seems to be subordinator approximation (4): can this arise in some other model?

Acknowledgments. Thanks to Boris Pittel for extensive interactions regarding this project. Thanks to Serte Donderwinkel for pointing out a gap in an early version, and to Jim Pitman and David Clancy and Prabhanka Deka for helpful comments on early versions. For recent (May 2024) alternative proofs mentioned in the text we thank Brett Kolesnik, Luca Pratelli and Pietro Rigo, and in particular Alexander Iksanov, whose observation of the connection with regenerative composition structures may lead to interesting further results.

References

- [1] Romain Abraham, Jean-François Delmas, and Patrick Hoscheit. A note on the Gromov-Hausdorff-Prokhorov distance between (locally) compact metric measure spaces. *Electron. J. Probab.*, 18:no. 14, 21 pp., 2013.
- [2] Louigi Addario-Berry, Marie Albenque, Serte Donderwinkel, and Robin Khanfir. Refined Horton-Strahler numbers I: a discrete bijection, 2024. arXiv 2406.03025, 2024.
- [3] David Aldous. Asymptotic fringe distributions for general families of random trees. *Ann. Appl. Probab.*, 1(2):228–266, 1991.
- [4] David Aldous. The continuum random tree. II. An overview. In *Stochastic analysis (Durham, 1990)*, volume 167 of *London Math. Soc. Lecture Note Ser.*, pages 23–70. Cambridge Univ. Press, Cambridge, 1991.
- [5] David Aldous. The continuum random tree. III. *Ann. Probab.*, 21(1):248–289, 1993.
- [6] David Aldous. Probability distributions on cladograms. In *Random discrete structures (Minneapolis, MN, 1993)*, volume 76 of *IMA Vol. Math. Appl.*, pages 1–18. Springer, New York, 1996.
- [7] David Aldous, Svante Janson, and Xiaodan Li. The harmonic descent chain, 2024. arXiv 2405.05102, 2024.

- [8] David Aldous and Boris Pittel. The critical beta-splitting random tree I: Heights and related results. arXiv:2302.05066, 2023.
- [9] David J. Aldous. Stochastic models and descriptive statistics for phylogenetic trees, from Yule to today. *Statist. Sci.*, 16(1):23–34, 2001.
- [10] Jean Bertoin. Homogeneous fragmentation processes. *Probab. Theory Related Fields*, 121(3):301–318, 2001.
- [11] Jean Bertoin. *Random fragmentation and coagulation processes*, volume 102 of *Cambridge Studies in Advanced Mathematics*. Cambridge University Press, Cambridge, 2006.
- [12] Anna Brandenberger, Luc Devroye, and Tommy Reddad. The Horton-Strahler number of conditioned Galton-Watson trees. *Electron. J. Probab.*, 26:Paper No. 109, 29 pp., 2021.
- [13] Timothy M. Crowe, Rauri C.K. Bowie, Paulette Bloomer, Tshifhiwa G. Mandiwana, Terry A.J. Hedderson, Ettore Randi, Sergio L. Pereira, and Julia Wake-ling. Phylogenetics, biogeography and classification of, and character evolution in, gamebirds (Aves: Galliformes): effects of character exclusion, data partitioning and missing data. *Cladistics*, 22(6):495–532, 2006.
- [14] Michael Drmota. *Random trees. An interplay between combinatorics and probability*. SpringerWienNewYork, Vienna, 2009.
- [15] Michael Drmota and Bernhard Gittenberger. On the profile of random trees. *Random Structures Algorithms*, 10(4):421–451, 1997.
- [16] Thomas Duquesne and Jean-François Le Gall. Random trees, Lévy processes and spatial branching processes. *Astérisque*, 281:vi+147, 2002.
- [17] Rick Durrett. *Probability: theory and examples*, volume 31 of *Cambridge Series in Statistical and Probabilistic Mathematics*. Cambridge University Press, Cambridge, fourth edition, 2010.
- [18] Steven N. Evans. *Probability and real trees*, volume 1920 of *Lecture Notes in Mathematics*. Lectures from the 35th Summer School on Probability Theory held in Saint-Flour, July 6–23, 2005. Springer, Berlin, 2008.
- [19] Alex Figueroa, Alexander D. McKelvy, L. Lee Grismer, Charles D. Bell, and Simon P. Lailvaux. A species-level phylogeny of extant snakes with description of a new colubrid subfamily and genus. *PLOS ONE*, 11(9):e0161070, 2016.

- [20] James Allen Fill and Svante Janson. The sum of powers of subtree sizes for conditioned Galton-Watson trees. *Electron. J. Probab.*, 27:Paper No. 114, 77 pp., 2022.
- [21] James Allen Fill, Svante Janson, and Stephan Wagner. Conditioned Galton-Watson trees: The shape functional, and more on the sum of powers of subtree sizes. *La Matematica*, 2024.
- [22] Mareike Fischer, Lina Herbst, Sophie Kersting, Luise Kühn, and Kristina Wicke. *Tree balance indices: a comprehensive survey*. Springer, 2023. Draft available at arXiv 2109.12281.
- [23] Philippe Flajolet, Xavier Gourdon, and Philippe Dumas. Mellin transforms and asymptotics: harmonic sums. *Theoret. Comput. Sci.*, 144(1-2):3–58, 1995.
- [24] Alexander Gnedin and Alexander Iksanov. Regenerative compositions in the case of slow variation: a renewal theory approach. *Electron. J. Probab.*, 17:no. 77, 19, 2012.
- [25] Christina Goldschmidt. Scaling limits of random trees and random graphs. In *Random graphs, phase transitions, and the Gaussian free field*, volume 304 of *Springer Proc. Math. Stat.*, pages 1–33. Springer, Cham, 2020.
- [26] Christina Goldschmidt, Bénédicte Haas, and Delphin Sénizergues. Stable graphs: distributions and line-breaking construction. *Ann. H. Lebesgue*, 5:841–904, 2022.
- [27] Morris Goodman, Lawrence I. Grossman, and Derek E. Wildman. Moving primate genomics beyond the chimpanzee genome. *TRENDS in Genetics*, 21(9):511–517, 2005.
- [28] Ronald L. Graham, Donald E. Knuth, and Oren Patashnik. *Concrete mathematics*. A foundation for computer science. Addison-Wesley Publishing Company, Reading, MA, second edition, 1994.
- [29] Geoffrey R. Grimmett and David R. Stirzaker. *Probability and random processes*. Oxford University Press, New York, third edition, 2001.
- [30] Bénédicte Haas and Grégory Miermont. Scaling limits of Markov branching trees with applications to Galton-Watson and random unordered trees. *Ann. Probab.*, 40(6):2589–2666, 2012.
- [31] Bénédicte Haas, Grégory Miermont, Jim Pitman, and Matthias Winkel. Continuum tree asymptotics of discrete fragmentations and applications to phylogenetic models. *Ann. Probab.*, 36(5):1790–1837, 2008.

- [32] Oskar Hagen, Klaas Hartmann, Mike Steel, and Tanja Stadler. Age-dependent speciation can explain the shape of empirical phylogenies. *Systematic Biology*, 64:432–440, 2015.
- [33] Inge S. Helland. Central limit theorems for martingales with discrete or continuous time. *Scand. J. Statist.*, 9(2):79–94, 1982.
- [34] Benjamin Hollering and Seth Sullivant. Exchangeable and sampling-consistent distributions on rooted binary trees. *J. Appl. Probab.*, 59(1):60–80, 2022.
- [35] Cecilia Holmgren and Svante Janson. Fringe trees, Crump-Mode-Jagers branching processes and m -ary search trees. *Probab. Surv.*, 14:53–154, 2017.
- [36] Alexander Iksanov. A comment on the article ‘The harmonic descent chain’ by D. J. Aldous, S. Janson and X. Li. Unpublished, 2024.
- [37] Alexander Iksanov. Another proof of CLT for critical beta-splitting tree. Unpublished, 2024.
- [38] Jasper Ischebeck. Central limit theorems for fringe trees in Patricia tries. arXiv 2305.14900, 2023.
- [39] Svante Janson. Tree limits and limits of random trees. *Combin. Probab. Comput.*, 30(6):849–893, 2021.
- [40] Svante Janson. Fringe trees of Patricia tries and compressed binary search trees. arXiv 2405.01239, 2024.
- [41] Brett Kolesnik. Critical beta-splitting, via contraction. arXiv 2404.16021, 2024.
- [42] Amaury Lambert. Probabilistic models for the (sub)tree(s) of life. *Braz. J. Probab. Stat.*, 31(3):415–475, 2017.
- [43] Jean-François Le Gall and Grégory Miermont. Scaling limits of random trees and planar maps. In *Probability and statistical physics in two and more dimensions*, volume 15 of *Clay Math. Proc.*, pages 155–211. Amer. Math. Soc., Providence, RI, 2012.
- [44] Heather R.L. Lerner and David P. Mindell. Phylogeny of eagles, Old World vultures, and other Accipitridae based on nuclear and mitochondrial DNA. *Molecular Phylogenetics and Evolution*, 37(2):327–346, 2005.
- [45] Harald Letsch. *Phylogeny of Anisoptera (Insecta: Odonata): promises and limitations of a new alignment approach*. PhD thesis, Rheinische Friedrich-Wilhelms-Universität in Bonn, 2007.

- [46] Russell Lyons and Yuval Peres. *Probability on trees and networks*, volume 42 of *Cambridge Series in Statistical and Probabilistic Mathematics*. Cambridge University Press, New York, 2016.
- [47] Alexandra Magro, E. Lecompte, F. Magne, J.-L. Hemptinne, and B. Crouau-Roy. Phylogeny of ladybirds (Coleoptera: Coccinellidae): are the subfamilies monophyletic? *Molecular Phylogenetics and Evolution*, 54(3):833–848, 2010.
- [48] Hosam M. Mahmoud. *Pólya urn models*. Texts in Statistical Science Series. CRC Press, Boca Raton, FL, 2009.
- [49] Ralph Neininger and Ludger Rüschendorf. On the contraction method with degenerate limit equation. *Ann. Probab.*, 32(3B):2838–2856, 2004.
- [50] Frank W. J. Olver, Daniel W. Lozier, Ronald F. Boisvert, and Charles W. Clark, editors. *NIST handbook of mathematical functions*. U.S. Department of Commerce, National Institute of Standards and Technology, Washington, DC; Cambridge University Press, Cambridge, 2010.
Also available as *NIST Digital Library of Mathematical Functions*, <http://dlmf.nist.gov/>
- [51] Matt Pennell. Alternate histories in macroevolution. *Proceedings of the National Academy of Sciences*, 120(9):e2300967120, 2023.
- [52] J. Pitman. *Combinatorial stochastic processes*, volume 1875 of *Lecture Notes in Mathematics*. Lectures from the 32nd Summer School on Probability Theory held in Saint-Flour, July 7–24, 2002. Springer-Verlag, Berlin, 2006.
- [53] Frederick H. Sheldon, Linda A. Whittingham, Robert G. Moyle, Beth Slikas, and David W. Winkler. Phylogeny of swallows (Aves: Hirundinidae) estimated from nuclear and mitochondrial DNA sequences. *Molecular Phylogenetics and Evolution*, 35(1):254–270, 2005.
- [54] Zhan Shi. *Branching random walks*, volume 2151 of *Lecture Notes in Mathematics*. Lecture notes from the 42nd Probability Summer School held in Saint Flour, 2012. Springer, Cham, 2015.
- [55] Mike Steel. *Phylogeny—discrete and random processes in evolution*, volume 89 of *CBMS-NSF Regional Conference Series in Applied Mathematics*. Society for Industrial and Applied Mathematics (SIAM), Philadelphia, PA, 2016.
- [56] Ximena Vélez-Zuazo and Ingi Agnarsson. Shark tales: a molecular species-level phylogeny of sharks (Selachimorpha, Chondrichthyes). *Molecular Phylogenetics and Evolution*, 58(2):207–217, 2011.

- [57] Alan T. Whittemore, Ryan S. Fuller, Bethany H. Brown, Marlene Hahn, Linus Gog, Jaime A. Weber, and Andrew L. Hipp. Phylogeny, biogeography, and classification of the elms (*Ulmus*). *Systematic Botany*, 46(3):711–727, 2021.
- [58] Timothy F. Wright, Erin E. Schirtzinger, Tania Matsumoto, Jessica R. Eberhard, Gary R. Graves, Juan J. Sanchez, Sara Capelli, Heinrich Müller, Julia Scharpegge, Geoffrey K. Chambers, Robert C. Fleischer. A multilocus molecular phylogeny of the parrots (Psittaciformes): support for a Gondwanan origin during the Cretaceous. *Molecular Biology and Evolution*, 25:2141–2156, 2008.
- [59] Chi Xue, Zhiru Liu, and Nigel Goldenfeld. Scale-invariant topology and bursty branching of evolutionary trees emerge from niche construction. *Proceedings of the National Academy of Sciences*, 117:7879–7887, 2020.